

Identification and Optimization of Benzimidazole Sulfonamides as Orally Bioavailable Sphingosine 1-Phosphate Receptor 1 Antagonists with *In Vivo* Activity

Edward J Hennessy, Vibha B. Oza, Ammar Adam, Kate Byth, Lillian Castriotta, Gurmit Grewal, Geraldine Hamilton, Victor M Kamhi, Paula Lewis, Danyang Li, Paul D Lyne, Linda Oster, Michael T Rooney, Jamal C Saeh, Li Sha, Qibin Su, Shengua Wen, Yafeng Xue, and Bin Yang

J. Med. Chem., **Just Accepted Manuscript** • DOI: 10.1021/acs.jmedchem.5b01078 • Publication Date (Web): 20 Aug 2015

Downloaded from <http://pubs.acs.org> on August 24, 2015

Just Accepted

“Just Accepted” manuscripts have been peer-reviewed and accepted for publication. They are posted online prior to technical editing, formatting for publication and author proofing. The American Chemical Society provides “Just Accepted” as a free service to the research community to expedite the dissemination of scientific material as soon as possible after acceptance. “Just Accepted” manuscripts appear in full in PDF format accompanied by an HTML abstract. “Just Accepted” manuscripts have been fully peer reviewed, but should not be considered the official version of record. They are accessible to all readers and citable by the Digital Object Identifier (DOI®). “Just Accepted” is an optional service offered to authors. Therefore, the “Just Accepted” Web site may not include all articles that will be published in the journal. After a manuscript is technically edited and formatted, it will be removed from the “Just Accepted” Web site and published as an ASAP article. Note that technical editing may introduce minor changes to the manuscript text and/or graphics which could affect content, and all legal disclaimers and ethical guidelines that apply to the journal pertain. ACS cannot be held responsible for errors or consequences arising from the use of information contained in these “Just Accepted” manuscripts.



Identification and Optimization of Benzimidazole Sulfonamides as Orally Bioavailable Sphingosine 1-Phosphate Receptor 1 Antagonists with *in Vivo* Activity

Edward J. Hennessy,* Vibha Oza, Ammar Adam, Kate Byth, Lillian Castriotta, Gurmit Grewal, Geraldine A. Hamilton, Victor M. Kamhi, Paula Lewis, Danyang Li, Paul Lyne, Linda Öster,[†] Michael T. Rooney, Jamal C. Saeh, Li Sha, Qibin Su, Shengua Wen, Yafeng Xue,[†] and Bin Yang

Oncology iMed, Innovative Medicines and Early Development, AstraZeneca R&D Boston, 35 Gatehouse Drive, Waltham, MA 02451, USA

[†]*Discovery Sciences, Innovative Medicines and Early Development, AstraZeneca R&D Mölndal, S-43183, Mölndal, Sweden*

Abstract

We report here a novel series of benzimidazole sulfonamides that act as antagonists of the S1P₁ receptor, identified by exploiting an understanding of the pharmacophore of an HTS-derived series of compounds described previously. Lead compound **2** potently inhibits S1P-induced receptor internalization in a cell-based assay ($EC_{50} = 0.05 \mu\text{M}$), but has poor physical properties and metabolic stability. Evolution of this compound through structure-activity relationship development and property optimization led to *in vivo* probes such as **4**. However, this compound was unexpectedly found to be a potent CYP3A inducer in human hepatocytes, and thus further chemistry efforts were directed at addressing this liability. By employing a PXR reporter gene assay to prioritize compounds for further testing in human hepatocytes, we identified lipophilicity as a key molecular property influencing the likelihood of P450 induction. Ultimately, we have identified compounds such as **46** and **47**, which demonstrate the desired S1P₁ antagonist activity while having greatly reduced risk of CYP3A induction in humans. These compounds have excellent oral bioavailability in preclinical species, and exhibit pharmacodynamic effects of S1P₁ antagonism in several *in vivo* models

1
2
3 following oral dosing. Relatively modest antitumor activity was observed in multiple
4
5 xenograft models, however, suggesting that selective S1P₁ antagonists would have limited
6
7 utility as anticancer therapeutics as single agents.
8
9

10 11 **Introduction**

12
13
14 Sphingosine 1-phosphate (S1P), a signaling phospholipid found throughout blood and
15
16 bodily tissues, plays a role in a diverse variety of biological processes. Through its
17
18 interactions with a class of five G protein-coupled receptors (GPCRs) known as the S1P
19
20 receptors (S1P₁-S1P₅), S1P plays a role in cell proliferation and migration, cellular
21
22 architecture, and immune cell trafficking.¹ Accordingly, agents that are capable of
23
24 modulating the interactions of S1P with its receptors may have utility as therapeutics in a
25
26 variety of diseases such as diabetes, inflammatory disorders, and cancer.
27
28

29
30 FTY720 (fingolimod), a sphingolipid mimetic first described in 1995,² is
31
32 phosphorylated in cells to yield a potent agonist for four of the five isoforms of S1P receptor
33
34 (S1P₁, S1P₃, S1P₄, and S1P₅).^{3,4} Through its interactions with S1P₁, this compound inhibits
35
36 lymphocyte egress from secondary lymphoid organs, resulting in an immunosuppressive
37
38 effect *in vivo*. As a result, it was approved for use in treatment of multiple sclerosis in 2010.⁵
39
40 Upon binding to and activating S1P₁, fingolimod causes prolonged downregulation of the
41
42 receptor by inducing receptor internalization⁶ followed by ubiquitinylation and proteasomal
43
44 degradation.^{7,8} Therefore, despite being an S1P₁ agonist, it is this “functional antagonism”
45
46 that is responsible for the compound’s beneficial therapeutic activity.
47
48

49
50 In addition to the effects on lymphocyte trafficking attributed to S1P₁ function, this
51
52 receptor has been shown to play a key role in angiogenesis and the maintenance of vascular
53
54 integrity. For example, S1P₁-knockout mice demonstrate impaired vascular maturation
55
56 during embryonic development, leading to lethal hemorrhaging *in utero*.⁹ Additionally,
57
58
59
60

1
2
3 siRNA silencing of the S1P₁ gene within subcutaneous implants of Matrigel results in the
4 suppression of vessel formation *in vivo*.¹⁰ Furthermore, small-molecule abrogation of S1P₁
5 signaling (with fingolimod) inhibits angiogenesis in multiple *in vivo* models.¹¹
6
7

8
9
10 In clinical trials of fingolimod, transient bradycardia was frequently observed upon
11 initial dosing.¹² This effect has also been observed preclinically in rodents, and has been
12 attributed to the compound's effects on the S1P₃ receptor.^{13,14} Alternative findings suggest
13 that S1P₁ agonism, resulting in activation of G protein-coupled inwardly rectifying potassium
14 (GIRK) channels in mouse¹⁵ and human cardiomyocytes,¹⁶ results in the heart rate decreases
15 observed in human patients.¹⁶ Taken together, these observations suggest that a compound
16 that selectively and effectively antagonizes the S1P₁ receptor, without any agonism of S1P₁
17 or interaction with S1P₃, should retain the desired pharmacological profile of fingolimod
18 without any adverse cardiovascular effects.
19
20
21
22
23
24
25
26
27
28

29
30 Given the documented role of S1P₁ function on vessel formation, and the therapeutic
31 potential of compounds that inhibit angiogenesis in the treatment of various cancers, we
32 aimed to develop an orally bioavailable, selective S1P₁ antagonist to assess the feasibility of
33 such a compound as an antitumor agent. While numerous examples of S1P₁ agonists that act
34 as functional antagonists have been described,¹⁷ at the time we initiated our program only a
35 few reports of pure antagonists (devoid of agonist activity) were available.¹⁸⁻²⁰ As mimetics
36 of the phospholipid S1P, these compounds are useful tools but likely have limited utility as
37 orally available agents. More recently, however, disclosures of orally available, small-
38 molecule S1P₁ antagonists have emerged in the literature.²¹⁻²³ We have recently disclosed
39 our initial efforts towards this goal, having identified a series of heterocyclic sulfonamides
40 with submicromolar potency in a S1P₁ receptor internalization assay.²⁴ In this Article, we
41 will detail our further evolution of this series of compounds, culminating in the identification
42
43
44
45
46
47
48
49
50
51
52
53
54
55
56
57
58
59
60

1
2
3 of compounds (such as **46** and **47**) with promising biopharmaceutical properties that elicit *in*
4
5 *vivo* pharmacodynamic effects associated with antagonism of the S1P₁ receptor.
6
7

8 9 10 **Results and Discussion**

11 In our previous communication,²⁴ we highlighted the preliminary development of
12 structure-activity relationships in a series of triazole-containing sulfonamides, with the goal
13 of improving potency alongside physical properties and metabolic stability. These efforts
14 established that substitution at the 4- and 5-positions of the triazole ring with small alkyl
15 groups gave the most effective S1P₁ antagonists (Figure 1, R¹ and R²). As part of this work,
16 we generated data which suggested that the hydrogen bond acceptor at the 1-position of the
17 triazole ring is not required for interaction with the S1P₁ receptor, since the corresponding
18 imidazole in which the 1-position nitrogen atom has been deleted retains the antagonist
19 activity seen in the triazole. However, the acceptor at the 2-position appears to be critical for
20 binding, since the matched-pair imidazole was inactive in an assay measuring inhibition of
21 S1P-induced S1P₁ receptor internalization.²⁵ These observations were further supported by
22 data for other heterocycles in which the 2-position hydrogen bond acceptor was maintained
23 while the 1-position nitrogen atom was replaced with other heteroatoms. Unfortunately, the
24 above modifications resulted in poorer physical properties than for the corresponding
25 triazoles.
26
27
28
29
30
31
32
33
34
35
36
37
38
39
40
41
42
43
44

45 To capitalize on these findings, we proposed additional structural modifications to the
46 triazole scaffold in order to assess the potential for improvements in potency and properties.
47 In particular, we hypothesized that a bicyclic system (such as benzimidazole) encompassing
48 the 5-position substituent as well as the 2-position hydrogen bond acceptor would maintain
49 the critical elements of the pharmacophore, while offering additional opportunities for further
50 substitution that could influence receptor binding as well as physical properties (Figure 1).
51
52
53
54
55
56
57
58
59
60

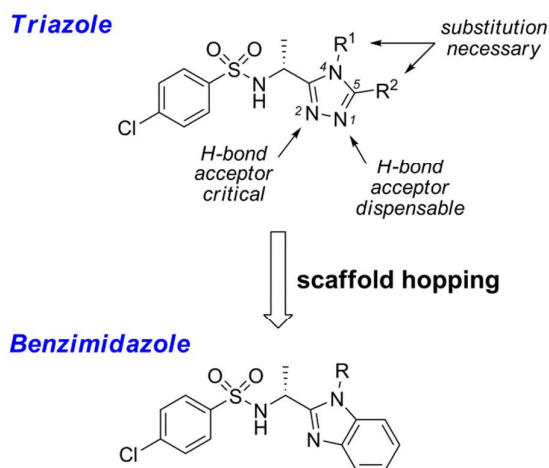
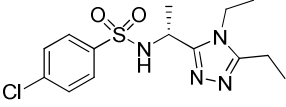
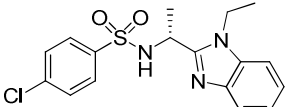


Figure 1. Scaffold hopping from triazole to benzimidazole core

To test this hypothesis, we first prepared benzimidazole **2** containing the structural elements found to be optimal from our studies on the triazole series (ethyl substituent off 5-membered ring, (*R*)-stereochemistry at chiral center).²⁴ We were pleased to find that this compound was a very effective antagonist of human SIP₁ in our receptor internalization assay, with improved measured potency relative to the most optimized triazoles previously prepared (exemplified by **1**, Table 1). No antagonism of the SIP₃ receptor was observed with this compound, consistent with our desired selectivity profile. Despite this promising result, however, this increased potency came at the cost of a significant increase in lipophilicity. Indeed, utilization of the lipophilic ligand efficiency (LLE) metric²⁶ indicates that triazole **1** is a far more “efficient” antagonist than benzimidazole **2**. Nevertheless, we were encouraged by the level of potency not yet observed in the project to that point, and viewed lipophilicity as a design parameter that could be readily addressed in future rounds of chemistry. We therefore embarked on efforts to establish the likelihood of delivery of a candidate drug from the benzimidazole scaffold.

Table 1. Comparison of lead triazole **1** with initial benzimidazole **2**

Example	Structure	S1P ₁ Translocation EC ₅₀ (μM) ^a	cLogP	LLE ^b
1		0.25 ± 0.037	2.1	4.5
2		0.05 ± 0.008	4.0	3.3

^aEC₅₀ values are reported as the mean of at least three separate determinations ± standard deviation; ^bLLE = pEC₅₀ – cLogP

An early goal of our work on this scaffold was to study the nature of the interaction between the compound and the receptor. The cellular S1P₁ translocation assay that we used for primary screening measures the effects of compound treatment on S1P-induced S1P₁ receptor internalization; compounds that behave as receptor agonists would be expected to increase the amount of receptor internalization relative to a fixed concentration of S1P alone, while antagonists should suppress receptor internalization. Based on our observations with **2**, we were confident that this compound was acting as an S1P₁ antagonist in the same manner as we had observed with the triazoles. In order to further characterize the mode of inhibition, we conducted this assay by varying the concentrations of S1P present at a series of fixed concentrations of **2**. Increasing the concentration of **2** results in a shift of the S1P agonism dose-response curve to the right, and also results in a decrease in the maximal amount of receptor internalization (Supporting Information, Figure S1). This observation, that antagonism by **2** cannot be overcome by increasing the concentration of S1P, suggests that **2** and S1P bind at different sites on the S1P₁ receptor, and that **2** is therefore a noncompetitive antagonist. We have observed a similar mode of inhibition with structurally-related compounds prepared previously (unpublished data).

Our initial investigations to follow up compound **2** focused on determining whether the structure-activity relationships previously established for the triazole series could be

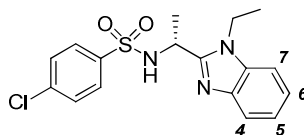
1
2
3 translated to this new scaffold. We therefore first systematically varied the group appended
4
5 to the benzimidazole nitrogen, including larger alkyl groups (linear and branched) as well as
6
7 substituents containing more polar moieties. However none of these compounds had
8
9 improved potency relative to **2** (data not shown), confirming the preference for ethyl
10
11 substitution at this position (in accord with our observations from the triazole series).²⁴
12
13 Similarly, exploration of substituents at the position adjacent to the sulfonamide nitrogen
14
15 reiterated our previous findings that an α -methyl group provided the most potency per unit
16
17 lipophilicity, and that (*R*)-stereochemistry at this position is critical to antagonist activity
18
19 (data not shown).
20
21

22
23 In spite of the observation that **2** represented a partially optimized early lead in this
24
25 series, this compound had apparent shortcomings that needed to be rectified. For example, **2**
26
27 is rapidly cleared *in vivo* when dosed intravenously to Wistar rats, and has very limited oral
28
29 exposure ($F\% = 5$). These observations are consistent with this compound's poor *in vitro*
30
31 stability in the presence of human liver microsomes ($CL_{int} > 100 \mu\text{L}/\text{min}/\text{mg}$). An analysis of
32
33 the metabolites formed in microsomal incubations pointed to *N*-deethylation of the
34
35 benzimidazole as the predominant product formed, along with compounds derived from
36
37 subsequent oxidation reactions.
38
39

40
41 Since our earlier data suggested that an *N*-ethyl group on the benzimidazole ring
42
43 seemed to be a critical component of the pharmacophore, modification of this group was not
44
45 considered to be a viable approach to address metabolic dealkylation. Instead, we next
46
47 focused our attention on the variation of substituents elsewhere on the scaffold. In addition to
48
49 the goal of furthering our understanding of structure-activity relationships within this series,
50
51 we hoped that microsomal stability data for successive compounds would point us towards
52
53 drivers for reducing the overall extent of oxidative metabolism.
54
55
56
57
58
59
60

1
2
3 A survey of various substitutions on the carbocyclic ring of the benzimidazole was
4
5 conducted, from which representative compounds are exemplified in Table 2. These data
6
7 highlight the effect of lipophilic groups on receptor antagonist activity. In particular, the
8
9 inclusion of small nonpolar groups at the 5- or 6-positions of this ring results in significant
10
11 increases in potency in the S1P₁ translocation assay relative to **2** (e.g., **3-5**), although in
12
13 general these improvements in potency do not offset the increased lipophilicity. As is the
14
15 case for **2**, these compounds have very limited stability in the presence of human
16
17 microsomes. Reducing lipophilicity by substitution of this ring with more polar groups does
18
19 appear to reduce the rate of metabolism *in vitro*, however more polar groups also tend to
20
21 result in a reduction in potency (**6-12**). A notable exception to this trend is the 6-
22
23 hydroxymethyl-substituted analog **8**, which has both a 10-fold improvement in potency
24
25 relative to **2** as well as ~1 log unit reduction in cLogP. Unfortunately, the microsomal
26
27 stability for this compound is still low, possibly due to the oxidation-prone benzylic alcohol
28
29 moiety. Substitution of the 7-position of this ring (as in compound **13**) results in a notable
30
31 drop in potency relative to **2**, which may be due to steric interactions adversely affecting the
32
33 orientation of the critical *N*-ethyl group.
34
35
36
37
38
39
40
41
42

Table 2. Representative substitutions on the benzimidazole ring



Example	Substitution	S1P ₁ Translocation EC ₅₀ (μM) ^a	cLogP	LLE ^b	Hu Microsomes CL _{int} (μL/min/mg)
3	6-OCH ₃	0.009 ± 0.009	4.2	3.8	>100
4	6-CF ₃	0.005 ± 0.004	4.9	3.4	>100
5	5-F, 6-Cl	0.001 ± 0.0001	4.9	4.1	>100
6	5-CN	0.13 ± 0.037	3.5	3.4	71
7	5-CH ₂ OH	0.18 ± 0.14	2.9	3.8	88
8	6-CH ₂ OH	0.005 ± 0.0005	2.9	5.4	84

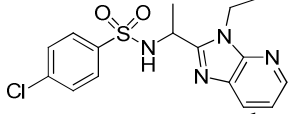
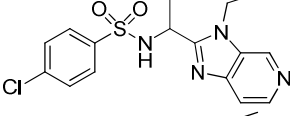
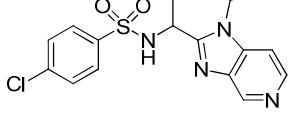
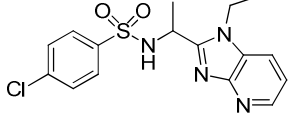
9	5-C(O)NH ₂	0.19 ± 0.037	2.9	3.8	<5
10	6-CH ₂ N(CH ₃) ₂	23.5 ± 2.9	3.8	0.8	30
11	5-morpholino	2.42 ± 0.81	3.8	1.8	45
12	6-SO ₂ CH ₃	1.84 ± 0.34	2.8	2.9	<5
13	7-Cl	0.80 ± 0.37	4.7	1.4	>100

^aEC₅₀ values are reported as the mean of at least three separate determinations ± standard deviation; ^bLLE = pEC₅₀ – cLogP

Since we observed a trend towards improved microsomal stability with decreasing lipophilicity of the benzimidazole substituent, we next surveyed the effects of incorporating a nitrogen atom into the benzimidazole 6-membered ring (Table 3). Due to the more forcing reaction conditions required to effect ring formation in these examples (as discussed in the Chemistry section), we decided to conduct this initial exploration with racemic compounds since our previous studies had shown that this tactic could be effectively applied to SAR development.²⁴ Gratifyingly, aza-substitution into this ring does not completely abrogate S1P₁ antagonism, with a clear preference for inclusion of nitrogen at the 5- and 4-positions of the benzimidazole (**16** and **17**, respectively). Moreover, a notable increase in microsomal stability was observed for these two compounds relative to **2**, reiterating our observations regarding the improved stability of compounds containing polar groups appended to this ring (Table 2). Not surprisingly, however, these compounds were found to have varying levels of cytochrome P450 inhibitory activity, likely owing to the iron-coordinating ability of the unhindered pyridine moiety.²⁷ For example, compound **16** inhibits both CYP2D6 (IC₅₀ = 0.23 μM) and CYP2C19 (IC₅₀ = 0.91 μM). Nevertheless, we were encouraged by the data for this initial set of azabenzimidazoles, and felt that these could be revisited at a later time as a means to potentially decrease lipophilicity and improve properties.

Table 3. Structure-activity relationships for racemic azabenzimidazoles

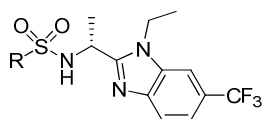
Example	Structure	S1P ₁ Translocation EC ₅₀ (μM) ^a	Hu Microsomes CL _{int} (μL/min/mg)
---------	-----------	---	---

14		2.34 ± 1.06	94
15		1.17 ± 0.34	93
16		0.21 ± 0.15	35
17		0.31 ± 0.09	15

^aEC₅₀ values are reported as the mean of at least three separate determinations \pm standard deviation

Earlier in the project, we had established that small, hydrophobic groups in the 3- and 4-positions of the aryl sulfonamide ring were critical to maintaining measurable antagonist activity, and the majority of our initial studies kept the 4-chlorophenylsulfonamide moiety as a constant to allow for direct comparisons between compounds with modifications elsewhere on the scaffold. Given the increased potency with benzimidazole **2**, however, we felt it was timely to challenge these prior assertions in the hopes that a less lipophilic sulfonamide group could be identified without resulting in a drastic loss of receptor antagonism. This work was well-suited to a parallel synthesis campaign, given the facile and high-yielding formation of the sulfonamide moiety (see Chemistry section). Therefore, employing the potent 6-trifluoromethyl-substituted compound **4** as a benchmark, we prepared a large number of compounds from readily available sulfonyl chlorides, representative examples of which are presented in Table 4.

Table 4. Effects of variation of the sulfonamide group



Example	R	S1P ₁ Translocation EC ₅₀ (μM) ^a	cLogP	LLE ^b	Hu Microsomes CL _{int} (μL/min/mg)
18		9.0 ± 4.2	2.6	2.4	<3
19		1.8 ± 0.52	3.5	2.2	not tested
20		0.008 ± 0.002	3.9	4.2	14
21		0.007 ± 0.008	4.4	3.8	26
22		0.024 ± 0.004	4.4	3.2	>100
23		0.012 ± 0.014	4.0	3.9	34
24		0.027 ± 0.005	4.9	2.7	>100
25		0.057 ± 0.022	4.0	3.2	>100
26		12.4 ± 5.1	3.1	1.8	>100
27		1.8 ± 0.45	5.9	-0.2	>100
28		0.24 ± 0.089	4.8	1.8	19

^aEC₅₀ values are reported as the mean of at least three separate determinations ± standard deviation; ^bLLE = pEC₅₀ - cLogP

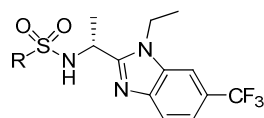
1
2
3 Analysis of the data for compounds in Table 4 reveals that while a range of
4
5 arylsulfonamides are tolerated, replacement of the aryl moiety with a cycloalkyl group (**18**,
6
7 **19**) results in a substantial loss of antagonist activity. With respect to substitution on the aryl
8
9 ring, the aforementioned preference for smaller, hydrophobic groups was reinforced here.
10
11 For example, the 4-fluoro, 4-methyl, and 4-cyano substituted compounds (**21**, **22**, and **23**,
12
13 respectively) have potency in the receptor internalization assay comparable to the 4-chloro
14
15 analog (**4**). Incorporation of these moieties at the 3-position (**24**, **25**) similarly results in
16
17 potent antagonists. Interestingly, even the unsubstituted phenyl sulfonamide **20** maintains
18
19 this level of potency. There do appear to be limitations with respect to the range of tolerated
20
21 substituents, however. For example, incorporation of a more polar amide group at the 4-
22
23 position (**26**) causes a >3000-fold drop in measured potency. In addition, while the 4-
24
25 isobutyl-substituted analog (**27**) is clearly outside the realm of acceptable lipophilicity, this
26
27 compound serves to illustrate that placement of larger groups on the aromatic ring results in a
28
29 loss of antagonist activity. Furthermore, comparison of the matched pair **21** and **28** highlights
30
31 that arenes without *ortho*-substituents are preferred.
32
33
34
35

36 The data in Table 4 also suggests that the substitution pattern on the sulfonamide ring
37
38 can address the issues of metabolic instability observed within this series. For example,
39
40 changing the 4-chlorophenyl ring of **4** to a 4-fluoro or 4-cyano-substituted aryl (**21** or **23**)
41
42 results in reduced human microsomal CL_{int}, as does removal of the 4-substituent altogether
43
44 (**20**). These improvements cannot be simply attributed solely to lipophilicity reduction,
45
46 however, as comparably polar compounds with moieties prone to benzylic oxidation (**22**, **26**)
47
48 have poorer stability.
49
50

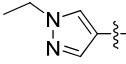
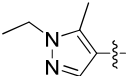
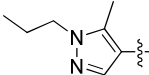
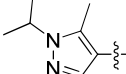
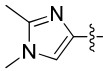
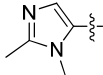
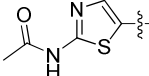
51 While some of the compounds prepared in this effort had improved LLE relative the 4-
52
53 chlorophenyl-substituted matched pair, we recognized that these compounds still were
54
55 relatively lipophilic in comparison to the triazole-based compounds. In order to introduce
56
57
58
59
60

more favorable physical properties, therefore, we prepared additional matched pairs of **4** containing heteroaryl sulfonamides (Table 5). Unfortunately, the majority these compounds were less effective antagonists than the corresponding arylsulfonamides. However, we were pleased to observe that the 3-pyridyl and 4-pyridyl analogs (**30** and **31**) did maintain the level of potency seen previously, suggesting that properties could be effectively attenuated with selected heterocyclic sulfonamides without a substantial loss in antagonist activity. Similar to our observations with the azabenzimidazoles (Table 3), however, these two compounds were found to be cytochrome P450 inhibitors (CYP3A4/5 IC_{50} for **30** = 0.83 μ M; CYP2C19 IC_{50} for **31** = 0.04 μ M).

Table 5. Exploration of heteroaryl sulfonamides



Example	R	S1P ₁ Translocation EC ₅₀ (μ M) ^a	cLogP	LLE ^b	Hu Microsomes CL _{int} (μ L/min/mg)
29		9.2 \pm 0.37	3.6	1.4	<3
30		0.030 \pm 0.005	3.5	4.0	>100
31		0.026 \pm 0.007	3.5	4.1	45
32		1.0 \pm 0.27	2.9	3.0	28
33		0.42 \pm 0.089	3.9	2.5	>100

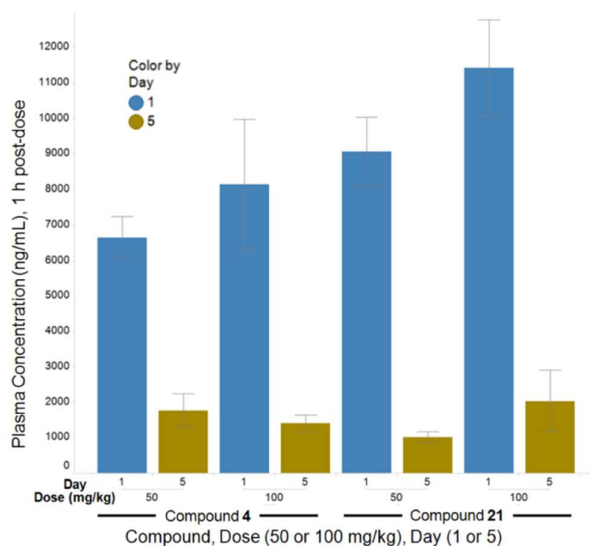
34		0.59 ± 0.080	3.2	3.0	95
35		0.43 ± 0.074	3.4	3.0	>100
36		0.80 ± 0.24	3.9	2.2	>100
37		1.1 ± 0.073	3.7	2.3	>100
38		4.0 ± 0.65	3.2	2.2	43
39		0.65 ± 0.15	3.1	3.1	58
40		2.2 ± 0.79	3.3	2.4	15

^aEC₅₀ values are reported as the mean of at least three separate determinations \pm standard deviation; ^bLLE = pEC₅₀ - cLogP

At the culmination of our investigation of various sulfonamide groups, the higher LLE compounds (such as **20**, **21**, and **23**) represented attractive candidates for exploratory *in vivo* studies. These examples were among the most effective antagonists in the receptor internalization assay prepared in the project at the time, and had improved microsomal stability relative to most other compounds of comparable potency. In addition, we were pleased to find that the instability of 4-chloro-substituted analog **4** in the presence of human microsomes (as well as human hepatocytes) did not translate to equally high turnover in mouse or rat hepatocytes. Indeed, **4** has moderate *in vivo* clearance (33 mL/min/kg) and acceptable oral bioavailability (43%) in rat. While metabolic instability in human would clearly preclude further progression of this compound, these data suggested that **4** might be a useful preclinical tool compound for rodent *in vivo* studies. Moreover, we profiled a number of the more potent compounds from this series (including **4** and **21**) in a cellular receptor

1
2
3 internalization assay using mouse S1P₁, and observed a correlation with potency in the
4
5 human S1P₁ assay (data not shown). Thus, we were confident that these compounds would
6
7 effectively act as S1P₁ antagonists in mice if sufficient plasma concentrations could be
8
9 achieved.
10

11
12 In preparation for *in vivo* experiments, we first wanted to accurately assess plasma
13
14 exposures at varying doses as well as tolerance of the animals to repeated dosing. Therefore,
15
16 compounds **4** and **21** were administered orally to mice at either 50 or 100 mg/kg, twice daily,
17
18 for a period of 5 days (Figure 2). We did not observe a significant increase in the plasma
19
20 exposure between the low and high dose for either compound, suggestive of poor solubility
21
22 and/or permeability limiting intestinal absorption for both compounds. More troubling,
23
24 however, we observed that plasma concentrations at 1 hour post-dose on day 5 were
25
26 markedly lower for both compounds than they were 1 hour post-dose on day 1.
27
28
29
30
31



32
33
34
35
36
37
38
39
40
41
42
43
44
45
46
47
48
49
50
51 **Figure 2.** Reduction in plasma exposures following repeat dosing. Female CB17 SCID mice
52 (3 animals per cohort) were dosed orally with either compound **4** or **21**, at either 50 mg/kg or
53 100 mg/kg twice daily, for 5 days. Plasma concentrations were measured at 1 hour after the
54 first dose on day 1 and day 5.
55
56
57
58
59
60

1
2
3 In order to address the observation of decreased exposures upon repeat dosing, we first
4 ruled out pharmaceutical properties of the compounds and formulations used. No
5 degradation or change in concentration of the oral formulations was observed over time for
6 either compound, nor was there any observable change in solid form or particle size by
7 microscopic assessment. As a result, we considered whether the decreased exposure of these
8 compounds was occurring through increased expression of the cytochrome P450 enzymes
9 responsible for their metabolism. While the detailed nature of the oxidative metabolism in
10 mouse was not evaluated for these compounds, we recognized that a possible P450 induction
11 liability with this series was something that needed to be identified and addressed
12 immediately. Otherwise, the risk of not being able to achieve sufficient, durable plasma
13 concentrations would hamper testing in relevant preclinical disease models and toxicological
14 studies. In addition, while it is known that there are substantial interspecies differences in the
15 regulation of cytochrome P450 enzymes,^{28,29} the possibility of a P450 induction risk in
16 humans (and the associated potential for adverse drug-drug interactions) would likely
17 preclude advancement of these compounds towards clinical development.

18
19
20
21
22
23
24
25
26
27
28
29
30
31
32
33
34
35
36 To determine if this series carried a risk for P450 induction in humans, cultured primary
37 human hepatocytes were treated with varying concentrations of **4** for a period of 48 hours,
38 and were then treated with probe substrates known to be metabolized by specific isoforms of
39 cytochrome P450 (Figure 3). No significant increase in CYP1A2 or CYP2B6 activity was
40 observed when compared to hepatocytes treated with compounds known to be inducers of
41 these enzymes. However, **4** was found to result in a dose-dependent increase in CYP3A
42 activity, with a concentration of 2 μ M resulting in an increase in metabolic activity
43 comparable to the reference compound rifampicin, a known potent inducer of CYP3A4 and
44 CYP3A5.³⁰

45
46
47
48
49
50
51
52
53
54
55
56
57
58
59
60

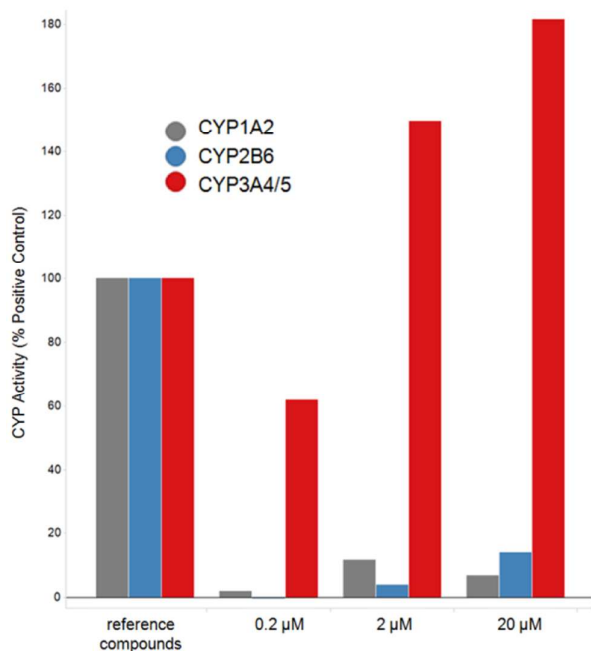


Figure 3. Compound **4** induces an increase in CYP3A activity in cultured human hepatocytes. Human hepatocytes were seeded onto collagen-coated plates and were cultured in a collagen-Matrigel sandwich configuration. On day 3 of culture, the cells were treated with either DMSO (control), compound **4**, or a reference compound known to cause induction of various CYP isoforms (3-methylcholanthrene for CYP1A2, phenobarbital for CYP2B6, and rifampicin for CYP3A4/5). After 48 hours of treatment, the cultures were then incubated with probe substrates (phenacetin for CYP1A2, bupropion for CYP2B6, and testosterone for CYP3A4/5), and the amount of marker metabolite formed (acetaminophen for CYP1A2, hydroxybupropion for CYP2B6, and 6- β -hydroxytestosterone for CYP3A4/5) was quantified. The amount of CYP activity for **4** is expressed as a percentage of the activity observed for the individual reference compounds.

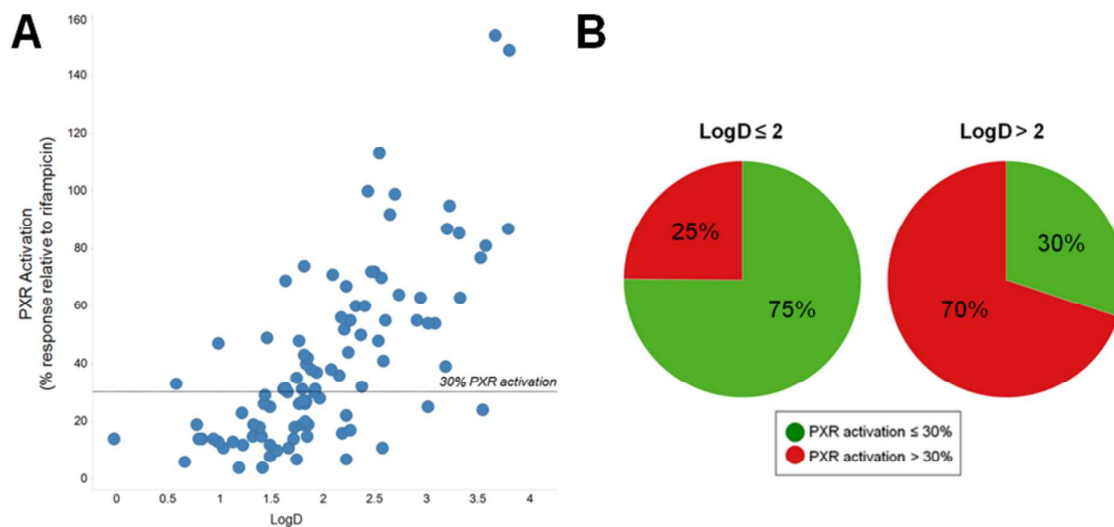
To determine whether these observations were specific to compound **4**, other compounds from this series were subsequently profiled in human hepatocytes, and similarly revealed varying degrees of increased CYP3A activity (data not shown). In light of these results, remediation of the human CYP3A induction liability within this series became the priority for ongoing chemistry activities. While the human hepatocyte activity protocol described in Figure 3 clearly indicated the magnitude of the issue, this assay wasn't considered to be suitable for routine screening purposes due to the labor intensive nature of the assay, as well as issues surrounding the availability and variable quality of human liver tissue. Therefore, we needed a higher throughput assay in order to identify design parameters

1
2
3 that would impact P450 induction, as well as to assess whether progress towards reducing
4
5 this liability was being made.
6

7
8 It has been established that compounds affecting expression of the genes encoding
9
10 P450 enzymes can do so through interactions with certain nuclear hormone receptors, such as
11
12 the pregnane X receptor (PXR)³¹⁻³³ and the constitutive androstane receptor (CAR).³⁴ These
13
14 receptors recognize xenobiotics through direct or indirect binding interactions, and in turn
15
16 affect expression of the metabolic enzymes that result in the clearance of such compounds
17
18 from the body. Cell-based reporter gene assays that measure the increase in P450 gene
19
20 expression associated with PXR activation by small molecules have been described,^{32,35,36} and
21
22 our strategy therefore was to utilize such an assay as a filter to allow for prioritization of
23
24 compounds to be screened for P450 activity in human hepatocytes. While the generation of
25
26 EC₅₀ values for PXR activation, derived from multiple concentrations of each compound,
27
28 would allow for rigorous rank-ordering of the compounds with respect to CYP3A induction
29
30 risk, we instead opted to evaluate the extent of PXR activation at a single concentration (10
31
32 μM) of each compound in order to generate a larger data set. The resulting data was
33
34 anticipated to help guide further compound design as well as to prioritize compounds for
35
36 further evaluation in human hepatocyte studies.
37
38
39

40
41 Upon screening a set of compounds from this series in a PXR gene reporter assay, we
42
43 observed a loose correlation between the extent of PXR activation (at 10 μM) and the
44
45 experimentally-determined LogD (Figure 4A), with more lipophilic compounds resulting in
46
47 greater PXR activation. This is in accord with previous literature observations, and is
48
49 consistent with more polar compounds having less favorable interactions with the relatively
50
51 hydrophobic binding site of PXR.³⁷ While there were compounds with lower LogD that did
52
53 result in significant PXR activation, it was clear from this data that the more lipophilic
54
55 compounds tested had an increased likelihood of this unwanted activity (and to a greater
56
57
58
59
60

1
2
3 extent). Indeed, roughly 70% of the compounds with $\text{LogD} > 2$ had $>30\%$ PXR activation at
4
5 a concentration of $10\ \mu\text{M}$ (relative to rifampicin), a threshold considered to be indicative of a
6
7 high risk of CYP3A induction in humans (Figure 4B).³⁷
8
9
10



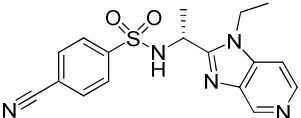
30
31 **Figure 4.** (A) Correlation between experimentally-determined LogD and extent of PXR
32 activation. Compounds with greater than 30% PXR activation at $10\ \mu\text{M}$ were considered to
33 be at risk for CYP3A induction. (B) Compounds with $\text{LogD} > 2$ are more likely to have
34 $>30\%$ PXR activation at $10\ \mu\text{M}$.
35
36

37
38 Given the LogD range that these data suggested would afford the best chance of
39
40 induction-free compounds, we stringently employed calculated lipophilicity as a primary
41
42 filter for all newly proposed compounds prior to initiating synthesis. In order to drive down
43
44 lipophilicity without sacrificing the potent S1P₁ antagonism within this series, we assessed
45
46 which previous structural permutations resulted in increased LLE, and utilized this
47
48 information to design compounds that combined such modifications. Therefore, based on the
49
50 promising data presented in Table 3, the focus of our efforts centered on revisiting
51
52 azabenzimidazoles. In particular, we felt that compounds in which the 5-position was a
53
54 nitrogen (as in **16**) would largely retain potency while effectively lowering lipophilicity. In
55
56 addition, the exploration around the aryl sulfonamide ring (Table 4) suggested the 4-cyano
57
58
59
60

group (as in **23**) contributed the least lipophilicity amongst the higher LLE compounds. Combining these groups gave **41** (Table 6), a compound that validated our design strategy to address P450 induction, combining potent antagonist activity with decreased activation of PXR. Given the low LogD for this compound, we hypothesized that addition of a moderately hydrophobic substituent at the 6-position would further enhance potency while staying within the desired property space. Moreover, we anticipated that the inclusion of a substituent at this position, adjacent to the pyridyl nitrogen, might attenuate the P450 inhibitory activity observed previously with azabenzimidazole-based compounds. Thus, we prepared **42-44**, and were pleased to find that these compounds had measured potency comparable to previous leads (**4** and **21**), but with reduced LogD and PXR activation.

In addition to the compounds resulting from these combinations, we were able to further exploit our previous finding that 3- or 4-pyridyl groups were tolerated as replacements for the substituted phenylsulfonamide (as shown in Table 5). In particular, the 3-pyridyl moiety still allowed for the incorporation of a potency-boosting 4-substituent on this ring, and thus combination of all these features (3-pyridyl, 4-cyano arylsulfonamide; 6-substituted 5-azabenzimidazole) led to compounds such as **45-47**. These examples represent a substantial improvement in compound quality compared to our earlier lead **4**, demonstrating comparable potent SIP₁ antagonist activity while having a reduction in LogD of over two orders of magnitude.

Table 6. Compounds with reduced lipophilicity and PXR activation

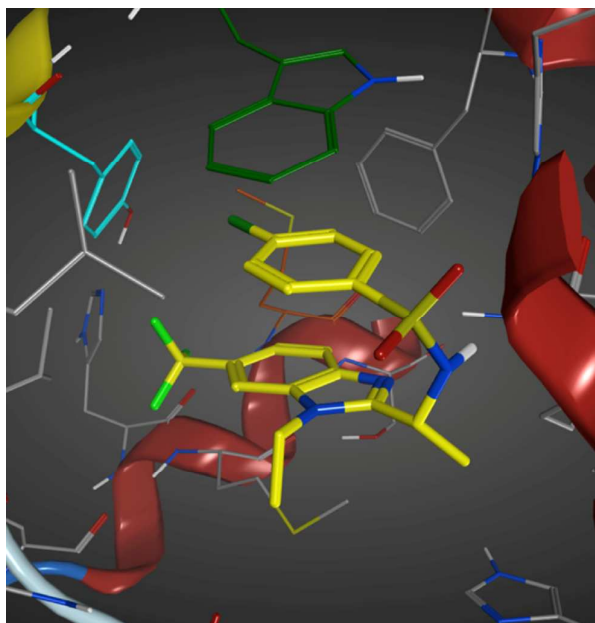
Example	Structure	SIP ₁ Translocation EC ₅₀ (μM) ^a	LogD ^b	PXR Activation ^c
41		0.034 ± 0.014	0.9	14

42		0.009 ± 0.004	1.4	18
43		0.003 ± 0.002	1.6	32
44		0.006 ± 0.005	1.9	27
45		0.028 ± 0.014	1.0	11
46		0.007 ± 0.005	1.3	15
47		0.004 ± 0.004	1.6	20

^aEC₅₀ values are reported as the mean of at least three separate determinations \pm standard deviation; ^bExperimentally determined at pH 7.4; ^cExpressed as a percentage of the activation response seen with rifampicin when both compounds are used at a concentration of 10 μ M.

Compounds **41-47** clearly demonstrate that the structure-activity relationships for interactions with SIP₁ and PXR can diverge, and that potent SIP₁ antagonists that do not substantially activate PXR are accessible from this series. To rationalize this observation and to potentially further inform our efforts at removing the CYP3A induction liability, we obtained a crystal structure of the potent inducer **4** bound to human PXR (Figure 5). The binding site occupied by this compound is indeed relatively nonpolar, and less lipophilic compounds would be expected to have fewer favorable hydrophobic interactions in general. In retrospect, however, our successful design approach to address PXR activation by lowering overall lipophilicity could have serendipitously impacted specific binding interactions with the receptor. For example, addition of a nitrogen atom at the 5-position of the benzimidazole (as in **41-47**) may disrupt contacts with the side chain of Met246. Alternatively, our decision to switch to 4-cyano-substituted sulfonamides in order to reduce

1
2
3 LogD may have resulted in unfavorable steric interactions with Tyr306 in PXR, manifesting
4
5 in reduced activation in the gene reporter assay. Interestingly, compound 4 binds to PXR in a
6
7 “bent-back” conformation, with the 4-chlorophenylsulfonamide group engaged in π -stacking
8
9 interactions with both the benzimidazole ring as well as the indole side chain of Trp299. It is
10
11 likely that the introduction of nitrogen atoms into the arylsulfonamide and benzimidazole
12
13 moieties would impact the electron density in these rings, possibly reducing the ability of
14
15 these groups to participate in such π -stacking³⁸ and resulting in decreased binding to the
16
17 receptor. Without detailed structural information regarding the nature of the interaction of
18
19 compounds from this series to S1P₁, however, the structural basis for these improvements in
20
21 PXR activation profile remains unclear.
22
23
24
25
26
27



28
29
30
31
32
33
34
35
36
37
38
39
40
41
42
43
44
45
46
47 **Figure 5.** Crystal structure of compound 4 bound to human PXR obtained at 2.3 Å resolution
48 (PDB ID 5A86). Coloration is as follows: compound 4 (yellow), Trp299 (green), Tyr306
49 (cyan), Met246 (brown).
50
51

52
53 Having identified a number of compounds with reduced PXR activation, we proceeded
54
55 to test whether these compounds in fact addressed the CYP3A induction liability in human
56
57 hepatocytes. At the time of our investigations, industry guidance on *in vitro* induction testing
58
59
60

1
2
3 had suggested that compounds that cause increased CYP3A activity (at concentrations
4 approximating an *in vivo* C_{max}) greater than 40% than that of rifampicin (at 10 μ M) were
5 considered to be at risk for induction *in vivo*.³⁹ A number of compounds meeting our PXR
6 activation criteria indeed resulted in <40% of the CYP3A activity caused by rifampicin in
7 human hepatocytes (Figure 6, blue circles). For compounds that did demonstrate increased
8 CYP3A activity (Figure 6, red circles), however, the single-point PXR activation assay was
9 largely unresponsive, as a number of compounds perceived to be low risk for induction did
10 carry this liability. This may be attributed, at least in part, due to the variability inherent in
11 using single point PXR activation data or hepatocyte studies using liver tissue from different
12 donors.⁴⁰ Alternatively, CYP3A induction resulting from activation of other xenobiotic
13 receptors (such as CAR) has not been considered in our approach. Nevertheless, we were
14 pleased to see that there were no “false negatives,” or compounds that were predicted to be
15 inducers in the PXR assay that did not show increased CYP3A activity. Thus, we felt
16 comfortable that by utilization of the PXR reporter gene assay at a single compound
17 concentration (instead of generating EC_{50} values) to prioritize compounds for further testing,
18 we had not unknowingly filtered induction-free compounds from further consideration.
19
20
21
22
23
24
25
26
27
28
29
30
31
32
33
34
35
36
37
38
39
40
41
42
43
44
45
46
47
48
49
50
51
52
53
54
55
56
57
58
59
60

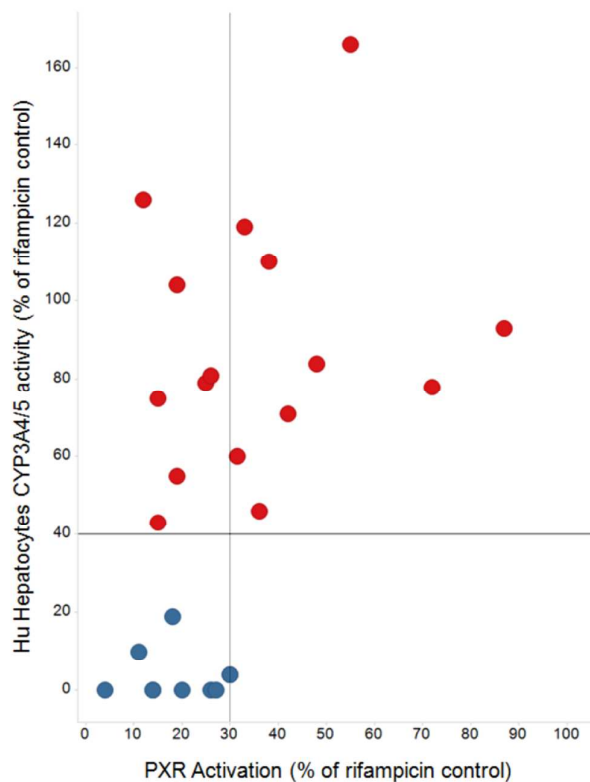


Figure 6. Correlation of PXR activation assay with CYP3A activity in human hepatocytes. Compounds with <40% CYP3A activity observed with rifampicin (both compounds at 10 μ M) are colored blue, while those with >40% activity are colored red.

At the culmination of our chemistry efforts, compounds **46** and **47** represented the top candidates for continued evaluation due to their potency, physical properties, and pharmacokinetic profiles in rat and dog (Table 7). These compounds did not show any measurable inhibition of the hERG channel or of any of the major P450 isoforms, and the human CYP3A induction risk was largely mitigated with compound **47**, which did not show any increase in CYP3A activity upon incubation with human hepatocytes. Compound **46** did show a borderline increase (43%) in CYP3A activity compared to rifampicin in hepatocytes from one donor, although on retest with a different batch of hepatocytes only a slight increase (5%) in CYP3A activity was observed. In repeat dosing experiments in mouse (at 20 mg/kg) and rat (at 25 mg/kg), neither compound showed appreciable decreases in plasma exposure (1 hour post-dose) between day 1 and day 5; higher doses (50 mg/kg) of these compounds in

mice did result in observable exposure decreases over time, with the effect more pronounced for **46** than for **47** (data not shown). Thus, despite known interspecies differences in xenobiotic-induced P450 upregulation, by addressing the human P450 induction liability in this series we had identified compounds and doses suitable for preclinical *in vivo* pharmacological and toxicological evaluation.

Table 7. Physical properties and pharmacokinetic parameters for compounds **46** and **47**

	Compound 46	Compound 47
Solubility (μM , pH 7.4)	765	>1000
Plasma Protein Binding (% free)	53 (mouse)	41 (mouse)
	32 (rat)	18 (rat)
	36 (dog)	50 (dog)
	24 (human)	19 (human)
Hepatocyte CL_{int} ($\mu\text{L}/\text{min}/10^6$ cells)	0.3 (mouse)	2.5 (mouse)
	2.1 (rat)	3.9 (rat)
	2.4 (dog)	1.7 (dog)
	1.2 (human)	0.2 (human)
CYP Inhibition (1A2, 2C9, 2C19, 2D6, 3A4/5) IC_{50}	all >20 μM	all >20 μM
hERG Inhibition (IC_{50})	>200 μM	>200 μM
Hu Hepatocyte CYP3A Induction (% activity compared to rifampicin)	5, 43 (results from two different donors)	0
<i>Rat pharmacokinetics</i>		
CL (mL/min/kg)	IV dosing, 3 mg/kg	IV dosing, 4 mg/kg
	8	10
	V_{dss} (L/kg)	1.2
$t_{1/2}$ (h)	2.4	2.9
C_{max} (μM)	PO dosing (10 mg/kg)	PO dosing (10 mg/kg)
	13.3	21.7
Bioavailability (F%)	87	93
<i>Dog pharmacokinetics</i>		
CL (mL/min/kg)	IV dosing, 2.5 mg/kg	IV dosing, 2 mg/kg
	2	2
	V_{dss} (L/kg)	0.6
$t_{1/2}$ (h)	4.9	4.6
	PO dosing (10 mg/kg)	PO dosing (5 mg/kg)

C_{\max} (μM)	31.1	10.7
Bioavailability (F%)	81	71

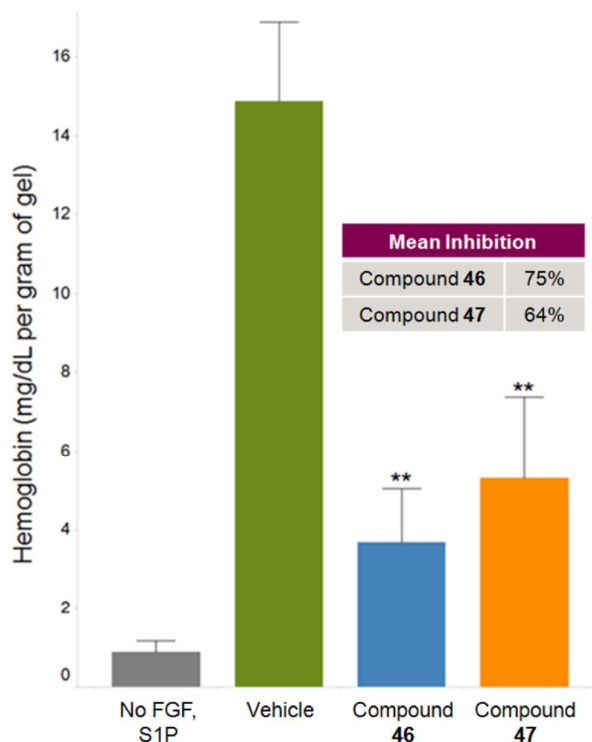


Figure 7. Inhibition of FGF/S1P-stimulated angiogenesis by compounds **46** and **47**. Matrigel (0.5 mL) containing 2 $\mu\text{g/mL}$ β -FGF and 1 μM S1P was injected subcutaneously into the ventral region of female 129s1/SvImJ mice. Compounds **46** and **47** were dosed orally at 10 mg/kg, once daily, on days 5-8 post-implant (5 animals per cohort). Plasma pharmacokinetics for both compounds was assessed 1 hour post-dose on day 4 (Supporting Information, Figure S2). The plugs were then harvested, and the amount of hemoglobin per gram of gel was quantified. Treated mice were compared with mice given vehicle used in the dosed groups (0.5% HPMC, 0.1% Tween 80) as a control, as well as mice injected with Matrigel not containing proangiogenic factors. The double asterisk (**) indicates $p < 0.01$.

To assess whether treatment with these compounds resulted in pharmacodynamic effects expected from S1P₁ antagonism *in vivo*, we utilized a previously-described Matrigel plug-based model that measured the ability of compounds to inhibit angiogenesis induced by FGF and enhanced by S1P (Figure 7).⁴¹ In the absence of these growth factors, very little angiogenesis (quantified by the amount of hemoglobin present in the Matrigel plug) occurs in

1
2
3 this model, whereas the combination of these results in the formation of well-developed
4
5 vessels.⁴¹ In control mice treated with vehicle only, this manifests as a significant increase in
6
7 hemoglobin content in the plug (Figure 7 and Supporting Information, Figure S3). When
8
9 mice are treated once daily with 10 mg/kg of either **46** or **47** for 4 days, a statistically
10
11 significant reduction in hemoglobin content within the plugs was observed compared to the
12
13 control group, consistent with these compounds acting as S1P₁ antagonists and suppressing
14
15 S1P-promoted angiogenesis. Similar observations have been made with S1P₁ siRNA in this
16
17 model.¹⁰
18
19

20
21 To further establish that our compounds were exerting pharmacological effects *in vivo*,
22
23 we determined whether they induced changes in capillary integrity using an Evans blue dye
24
25 lung leakage model. Evans blue dye (EBD) binds tightly to the albumin present in plasma,
26
27 and when vessel function is compromised an increase in EBD in tissue would be observed as
28
29 a result of leakage of plasma proteins from the vasculature. Several previous studies have
30
31 demonstrated an increase in EBD content in rodent lungs upon treatment with S1P₁
32
33 antagonists, suggesting these compounds cause an increase in pulmonary vascular
34
35 permeability.^{20,23,42} In our hands, when female NCr nude mice were treated orally with either
36
37 compound **46** (20 mg/kg) or **47** (50 mg/kg), plasma concentrations of both compounds at 1
38
39 hour post-dose are more than sufficient to expect target engagement based on *in vitro* potency
40
41 and relatively low plasma protein binding (Supporting Information, Figure S4). In this strain
42
43 of mice, these doses result in a substantial increase in EBD content in the lungs relative to
44
45 vehicle-treated controls (Figure 8 and Supporting Information, Figure S5), consistent with
46
47 these compounds acting as S1P₁ antagonists *in vivo*.
48
49
50
51
52
53
54
55
56
57
58
59
60

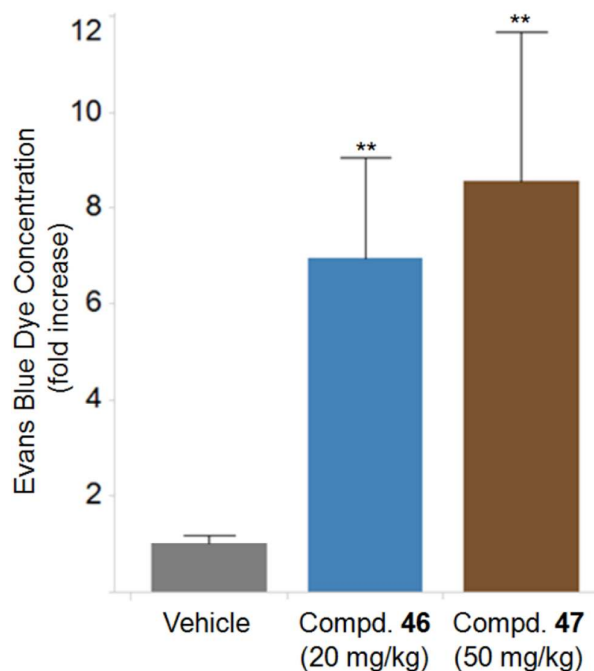


Figure 8. Induction of capillary leakage in mouse lungs by compounds **46** and **47**. Female NCr nude mice (4 animals per cohort) were dosed orally with either compound **46** (20 mg/kg), compound **47** (50 mg/kg), or vehicle alone (0.5% HPMC, 0.1% Tween 80). After 1 hour, the mice were injected with a solution of Evans blue dye (20 mg/kg). After an additional 30 minutes, the mice were anesthetized and perfused with 0.9% normal saline. The lungs were harvested, and the amount of Evans blue dye present was determined by spectrophotometry. The amount of dye present was normalized to the amount found in vehicle-treated animals. The double asterisk (**) indicates $p < 0.005$.

Having demonstrated that oral doses of compounds **46** and **47** achieve plasma concentrations that result in functional effects related to S1P₁ antagonism, we next assessed whether these compounds were efficacious in tumor xenograft studies. A number of xenograft models were explored, with a focus on those in which previous antiangiogenic agents have demonstrated effects on tumor vasculature.^{43,44} Despite the observations of *in vivo* activity described above, only modest antitumor activity was observed with our compounds across the models evaluated. For example, compound **47** demonstrated 32% tumor growth inhibition in a Calu6 xenograft model when dosed orally at 50 mg/kg twice daily, while compound **46** (at 20 mg/kg twice daily) did not result in statistically significant reductions in tumor volume (Figure 9). In contrast to the observation of marked increases in

capillary leakiness in murine lungs, we did not observe statistically significant increases in EBD accumulation in tumor tissue obtained from either Calu6 or Colo205 xenograft-bearing mice treated with these compounds (data not shown), suggesting that these agents do not substantially affect vascular integrity within the tumor. Even though decreases in plasma exposure (1 hour post-dose) over time were observed with **47**, both compounds achieved plasma exposures throughout the duration of these studies comparable to those observed in the previously-described *in vivo* experiments (Supporting Information, Figure S6). Therefore, given the disparity between the activity we observed in the pharmacodynamic models and the various tumor xenograft studies, we conclude that a selective S1P₁ antagonist would have only minimal effects on tumor growth inhibition as a single agent.

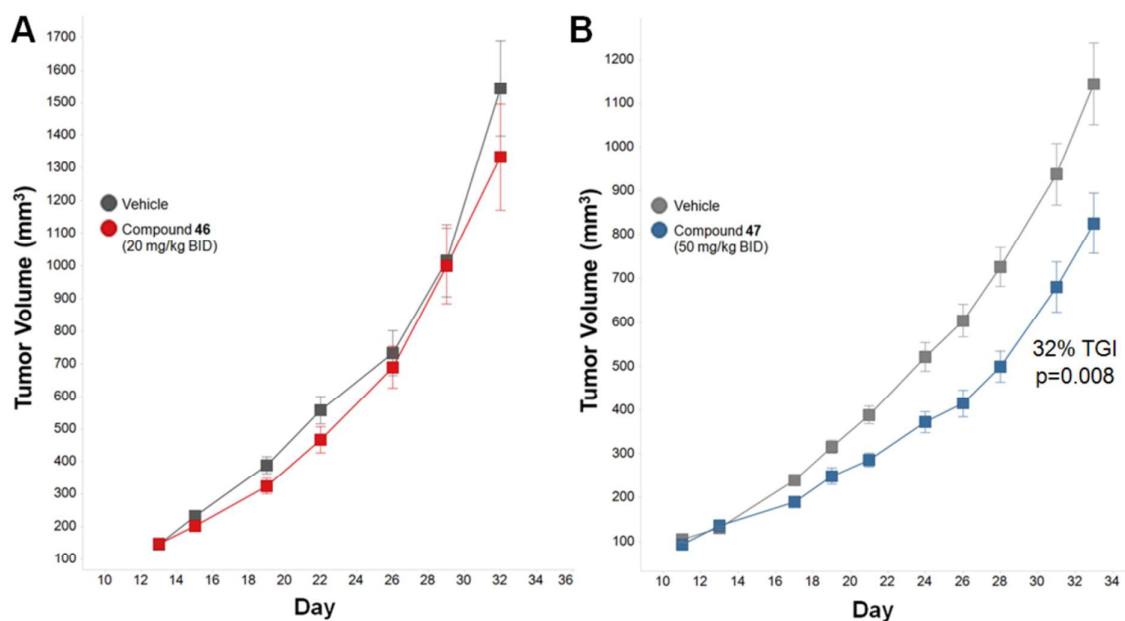
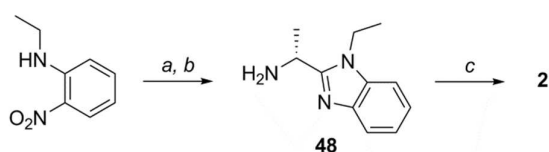


Figure 9. Evaluation of antitumor activity of lead S1P₁ antagonists in a Calu6 xenograft model in female Ncr-nude mice. (A) Compound **46**, dosed orally at 20 mg/kg BID (n=14) on days 13-32, does not result in statistically significant tumor growth inhibition relative to vehicle (HPMC)-treated controls (n=20). (B) Compound **47**, dosed orally at 50 mg/kg BID (n=14) on days 11-33, results in 32% tumor growth inhibition (p=0.008) relative to controls (n=20).

Chemistry

The benzimidazole sulfonamides discussed in this paper were prepared as described in the schemes below. The sulfonamide moiety was typically installed in the last step, by the reaction of the chiral amine with commercially available or readily prepared sulfonyl chlorides. The amine reactant was derived from the cyclocondensation of an appropriately substituted aromatic diamine with an alanine derivative. For example, benzimidazole **2** was obtained by refluxing *N*-ethyl-1,2-phenylenediamine and D-alanine in 6 N HCl for several days, followed by coupling with 4-chlorobenzenesulfonyl chloride (Scheme 1).

Scheme 1. Preparation of benzimidazole **2**^a

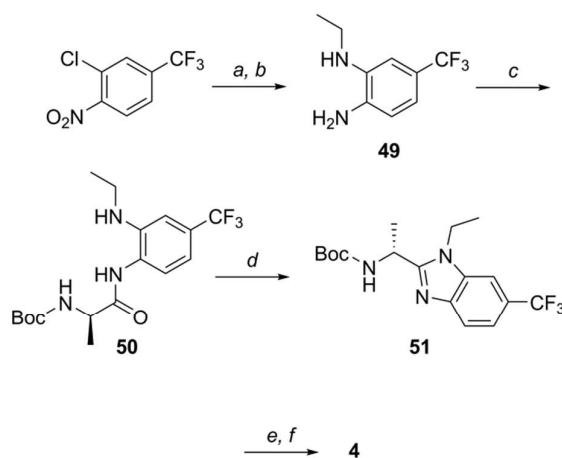


^aReagents and conditions: (a) Pd/C, H₂, EtOH, rt; (b) D-Ala-OH, 6N HCl, 100 °C; (c) 4-chlorobenzenesulfonyl chloride, NEt₃, CH₂Cl₂, 0 °C.

For the preparation of benzimidazoles containing substituents on the carbocyclic ring, it was necessary to obtain the appropriately substituted 1,2-phenylenediamine derivatives. While in principle the *N*-ethyl group could be installed following benzimidazole ring formation through alkylation, we were concerned about the prospect of inseparable mixtures of regioisomers and thus sought to install this group prior to cyclization. In many cases, this was conveniently achieved through nucleophilic aromatic substitution on a substituted *ortho*-halo nitroarene, followed by reduction of the nitro group (as in Scheme 2). Given the harsh cyclization conditions employed in the preparation of **2**, we chose to pursue a stepwise approach for future analogs to ensure functional group compatibility. Thus, using compound **4** as a representative example, coupling of the aryl diamine **49** with Boc-D-alanine under standard amide bond formation conditions yielded intermediate **50**. Cyclization to **51**

occurred with heating in glacial HOAc, avoiding excessive reaction temperatures in order to minimize Boc-deprotection or loss in optical activity. Removal of the Boc group followed by sulfonamide installation as above afforded the target compound. While other methods of benzimidazole formation were employed for select cases, the chemistry described in Scheme 2 could be readily applied to most of the compounds prepared in this series. Similarly, variation of the sulfonyl chloride used in the final step (with either commercially-available or previously described reagents) afforded the compounds depicted in Tables 4 and 5.

Scheme 2. Representative synthesis of a substituted benzimidazole sulfonamide^a



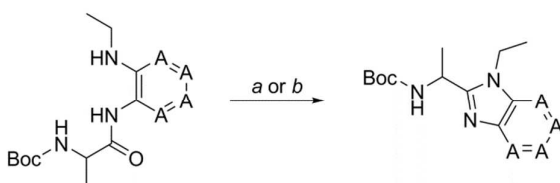
^aReagents and conditions: (a) ethylamine (2 M in THF), 100 °C (microwave irradiation); (b) 10% Pd/C, H₂, EtOH, rt; (c) Boc-D-Ala-OH, HATU, NEt₃, DMF, 0 °C to rt; (d) glacial HOAc, 65 °C; (e) 4 N HCl/dioxane, rt; (f) 4-chlorobenzenesulfonyl chloride, NEt₃, CH₂Cl₂, 0 °C.

For the preparation of azabenzimidazoles from pyridine-derived diamines (as for compounds **14-17**), the cyclization conditions described above were less effective. As a result, more forcing conditions needed to be employed. For instance, we found that even prolonged heating in refluxing acetic acid failed to convert any of the intermediate amide to the cyclized product. However, when heated at 150 °C under microwave irradiation, the desired products were isolable in low yield. Similarly, we found that the cyclization could be

1
2
3 effected at this high temperature using a stoichiometric amount of Lawesson's reagent.

4
5 Given the requisite forcing conditions, we intentionally prepared these initial compounds as
6
7
8
9
10
11
12
13
14
15
16
17
18
19
20
21
22
23
24
25
26
27
28
29
30
31
32
33
34
35
36
37
38
39
40
41
42
43
44
45
46
47
48
49
50
51
52
53
54
55
56
57
58
59
60
racemates to alleviate concerns over epimerization during the reaction.

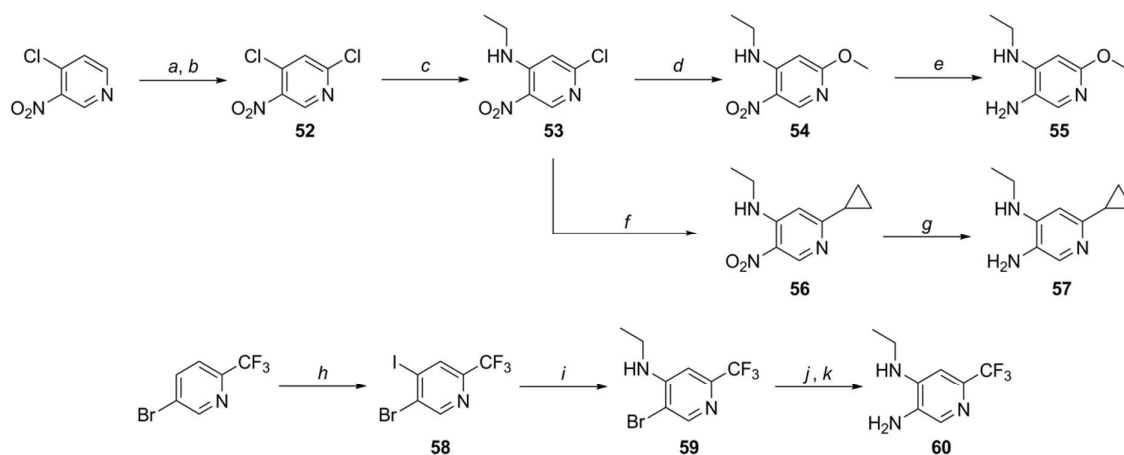
Scheme 3. Forcing conditions required for cyclization of azabenzimidazoles **14-17**^a



^aReagents and conditions: (a) glacial HOAc, 150 °C (microwave irradiation); (b) Lawesson's reagent, dioxane, 150 °C (microwave irradiation).

For the preparation of subsequent project compounds containing a substituted azabenzimidazole ring (Table 6), the requisite pyridine 3,4-diamines were obtained following the chemistry detailed in Scheme 4. Thus, the methoxy- and cyclopropyl-substituted pyridines were obtained from the common precursor **53**, which in turn was obtained from 4-chloro-3-nitropyridine through a sequence of vicarious nucleophilic substitution of hydrogen⁴⁵ followed by chlorination. To prepare the trifluoromethyl-substituted diamine **60**, 5-bromo-2-(trifluoromethyl)pyridine was deprotonated with LDA, and the resultant anion was quenched with iodine to give **58**. Displacement of the iodide with ethylamine afforded **59**, which was converted to the diamine **60** by palladium-catalyzed amination with benzophenone imine followed by hydrolysis.

Scheme 4. Preparation of diaminopyridine precursors to compounds **42-47**^a

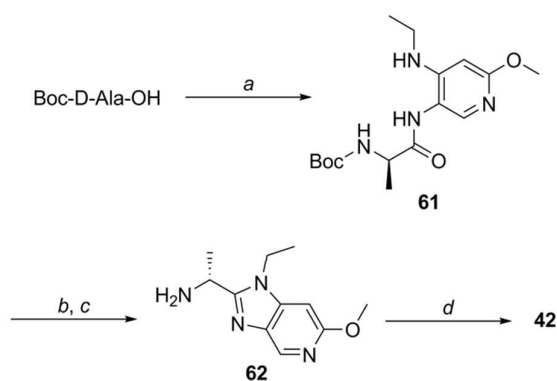


^aReagents and conditions: (a) Potassium *tert*-butoxide, *tert*-butylhydroperoxide (5 M in decane), NH₃(l), THF, -35 °C; (b) POCl₃, toluene, 100 °C; (c) ethylamine (2 M in THF), THF, 0 °C; (d) NaOMe, MeOH, 65 °C; (e) SnCl₂ • 2 H₂O, EtOAc, 80 °C; (f) cyclopropylboronic acid, Pd(PPh₃)₄, K₃PO₄, toluene, water, 100 °C; (g) H₂ (5 bar), 5% Pd/C, MeOH, rt; (h) LDA, THF, -78 °C, then I₂; (i) ethylamine (70% in water), EtOH, 80 °C; (j) benzophenone imine, sodium *tert*-butoxide, Pd₂(dba)₃, *rac*-BINAP, toluene, 110 °C; (k) 2 M HCl, THF, rt.

Because of the electron-deficient nature of these pyridine substrates, the standard amide bond coupling with Boc-D-alanine (as described in Scheme 2) proved to be troublesome and typically resulted in very low yields. In addition to concerns surrounding the stereochemical integrity of the chiral center that would result from more forcing conditions, most attempts to push these reactions to completion through heating often resulted in unwanted side products. For these particular substrates, we found it advantageous to generate the acylimidazolide of the protected amino acid, which in our hands seemed to be more stable towards gentle heating and resulted in minimal byproduct formation. Thus, pretreatment of Boc-D-alanine with CDI in CH₂Cl₂ followed by addition of the diaminopyridine (with heating to 40 °C if necessary) afforded the desired amide intermediates with no observable loss in optical activity (Scheme 5). Since the cyclization conditions described in Scheme 3 were anticipated to result in racemization, we sought to identify an alternative cyclization methodology for these electron-deficient substrates. Ultimately, we found that removal of the Boc-protecting group followed by heating under alkaline conditions yielded the cyclized benzimidazole with

1
2
3 minimal epimerization (the products isolated were typically 80-90% ee). Prolonged reaction
4
5 times for this cyclization resulted in further erosion in optical activity, and so reaction
6
7 progress was carefully monitored in each case. Following introduction of the sulfonamide
8
9 moiety, the enantiopure materials were obtained through chiral chromatography (to remove
10
11 the minor enantiomer) or by recrystallization.
12
13

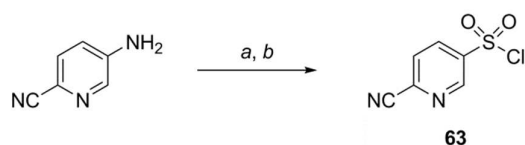
14
15
16 **Scheme 5.** Representative synthetic route to access substituted azabenzimidazoles^a
17



^aReagents and conditions: (a) CDI, CH₂Cl₂, rt, then **55**, rt; (b) 4 N HCl/dioxane, rt; (c) NaOH, EtOH, 80 °C; (d) 4-cyanobenzenesulfonyl chloride, NEt₃, CH₂Cl₂, 0 °C, then chiral chromatography.

For compounds **45-47**, the requisite sulfonyl chloride **63** was synthesized from 5-aminopicolinonitrile, through reaction of the corresponding diazonium hydrochloride salt with sulfur dioxide (prepared *in situ* by hydrolysis of thionyl chloride, Scheme 6).

46
47 **Scheme 6.** Preparation of sulfonyl chloride **63**^a
48



^aReagents and conditions: (a) conc. HCl, NaNO₂, water, 0 °C; (b) thionyl chloride, water, 0 °C, then CuCl, 0 °C.

Conclusions

We have discovered a novel class of benzimidazole sulfonamides that act as SIP₁ antagonists, by scaffold hopping from a lead series we have previously described. Our initial efforts in this series were directed at developing structure-activity relationships and at identifying drivers for improving overall metabolic stability. The early *in vivo* probe compounds thus obtained appeared to be inducers of metabolic enzymes in mouse, and in subsequent experiments demonstrated potent induction of CYP3A in human hepatocytes. In order to overcome this liability, we utilized a PXR reporter gene assay to prioritize compounds for assessment of CYP3A activity in human hepatocytes. Ultimately, by focusing on reducing compound lipophilicity through the introduction of polar moieties known to be tolerated within this scaffold, we have identified compounds (such as **46** and **47**) which are largely free of any human P450 induction issues. These compounds both show indirect evidence of target engagement *in vivo* when dosed orally, exhibiting pharmacodynamic effects consistent with previously described SIP₁ antagonists. In a variety of xenograft models, we did not see any evidence of antiangiogenic effects in tumor tissue, and only modest antitumor activity was observed. Taken together, these data suggest that selective SIP₁ antagonists would not have significant activity as single agent anticancer therapeutics.

Experimental Section

All reagents and solvents used were purchased from commercial sources and were used without further purification. ¹H NMR spectra were obtained using a Bruker 300 MHz or 400 MHz spectrometer at room temperature; chemical shifts are expressed in parts per million (ppm, δ units) and are referenced to the residual protons in the deuterated solvent used.

1
2
3 Coupling constants are given in units of hertz (Hz). Splitting patterns describe apparent
4 multiplicities and are designated as s (singlet), d (doublet), t (triplet), q (quartet), m
5 (multiplet), and br s (broad singlet). Mass spectrometry analyses were performed with an
6 Agilent 1100 equipped with Waters columns (Atlantis T3, 2.1x50 mm, 3 μ m; or Atlantis
7 dC18, 2.1 x 50 mm, 5 μ m) eluted with a gradient mixture of water and acetonitrile with either
8 formic acid or ammonium acetate added as a modifier. Reverse-phase chromatography was
9 performed on a Gilson system using an Atlantis Prep T3 OBD reverse-phase HPLC column
10 (19 mm x 100 mm) in water/MeCN with 0.1% TFA as mobile phase. Thin layer
11 chromatography was performed using EMD silica gel 60 F₂₅₄ plates, which were visualized
12 using UV light. Column chromatography was performed using SiliCycle SiliaSep preloaded
13 silica gel cartridges on Teledyne ISCO CombiFlash Companion automated purification
14 systems. All final compounds were purified to \geq 95% purity as assessed by analytical HPLC
15 using an Agilent 1100 equipped with Waters columns (Atlantis T3, 2.1x50 mm, 3 μ m; or
16 Atlantis dC18, 2.1 x 50 mm, 5 μ m) eluted for > 10 minutes with a gradient mixture of water
17 and acetonitrile with either formic acid or ammonium acetate added as a modifier, monitored
18 at wavelengths of 220, 254, and 280 nm. All *in vivo* experiments described in this article
19 were conducted in accordance with the Institute for Laboratory Animal Research Guide for
20 the Care and Use of Laboratory Animals, and within the protocols approved by the Institute
21 of Animal Care and Use Committee at AstraZeneca.

22
23
24
25
26
27
28
29
30
31
32
33
34
35
36
37
38
39
40
41
42
43
44
45 **(R)-1-(1-Ethyl-1H-benzo[d]imidazol-2-yl)ethanamine (48):** To a solution of 1-ethyl-
46 2-nitroaniline (5.0 g, 30.0 mmol) in EtOH (100 mL) was added 10% Pd on carbon (1.24 g).
47 The mixture was hydrogenated in a Parr apparatus under 50 psi of H₂ gas for 2 hours, and the
48 resulting mixture was filtered through Celite. The filter cake was washed with EtOAc, and
49 the combined filtrates were concentrated under reduced pressure to give the diamine as
50 brown oil (4.0 g, quantitative). ¹H NMR (300 MHz, CDCl₃) δ ppm 1.28 (t, *J*=7.1 Hz, 3H),
51
52
53
54
55
56
57
58
59
60

1
2
3 3.12-3.19 (m, 5H), 6.68-6.72 (m, 4H). LC-MS (M+H) 137. A mixture of this material (2.00
4 g, 14.7 mmol) and D-alanine (2.2 g, 22.0 mmol) in 6 N aqueous HCl (15.0 mL) was heated at
5 100 °C for a total of 6 days. The mixture was allowed to cool, was neutralized with 2 N
6 NaOH, and was extracted with EtOAc (3x50 mL). The combined organics were washed with
7 brine, dried (Na₂SO₄), filtered, and concentrated under reduced pressure. The crude material
8 was purified by silica gel chromatography (95:5 CHCl₃:MeOH) to give the title compound as
9 a brown oil (2.25 g, 81%). ¹H NMR (300 MHz, CDCl₃) δ ppm 1.45 (t, *J*=7.1 Hz, 3H), 1.61
10 (d, *J*=7.1 Hz, 3H), 1.81 (br. s., 2H), 4.17-4.36 (m, 3H), 7.21-7.37 (m, 3H), 7.72-7.78 (m, 1H).
11 LC-MS (M+H) 190.

22
23 **(*R*)-4-Chloro-N-(1-(1-ethyl-1*H*-benzo[d]imidazol-2-yl)ethyl)benzenesulfonamide**
24 **(2):** A solution of **48** (700 mg, 3.70 mmol) and NEt₃ (1.70 mL, 12.2 mmol) in CH₂Cl₂ (30
25 mL) was cooled to 0 °C. A solution of 4-chlorobenzenesulfonyl chloride (820 mg, 3.88
26 mmol) in CH₂Cl₂ (5 mL) was added dropwise, and the reaction mixture was allowed to stir at
27 room temperature overnight. The mixture was partitioned between CH₂Cl₂ and water, and
28 the organic layer was washed with brine and was then concentrated under reduced pressure.
29 The crude material was purified by silica gel chromatography (98:2 CHCl₃:MeOH) to give
30 the title compound as a solid (1.30 g, 97%). ¹H NMR (300 MHz, CDCl₃) δ ppm 1.35 (t,
31 *J*=7.1 Hz, 3H), 1.56 (d, *J*=6.9 Hz, 3H), 3.99-4.24 (m, 2H), 4.75-4.85 (m, 1H), 6.18 (d, *J*=8.3
32 Hz, 1H), 7.16-7.26 (m, 5H), 7.57-7.64 (m, 3H). LC-MS (M+H) 364.

33
34
35
36
37
38
39
40
41
42
43
44
45 **N1-Ethyl-5-(trifluoromethyl)benzene-1,2-diamine (49):** A microwave reaction tube
46 was charged with a stir bar and with 2-chloro-1-nitro-4-(trifluoromethyl)benzene (776 mg,
47 3.44 mmol). The tube was then charged with a 2 M MeOH solution of ethylamine (5.0 mL,
48 10.0 mmol), and was sealed and heated at 150 °C for 2 hours in a microwave reactor. The
49 resulting mixture was transferred to a roundbottom flask and was concentrated under reduced
50 pressure. The orange-yellow solid was partitioned between EtOAc and water, and the
51
52
53
54
55
56
57
58
59
60

1
2
3 aqueous layer was extracted with EtOAc. The combined organics were washed with brine
4
5 and were concentrated under reduced pressure to give the substituted 2-nitroaniline as a
6
7 yellow-orange solid (811 mg). ¹H NMR (400 MHz, DMSO-*d*₆) δ ppm 1.22 (t, *J*=7.1 Hz,
8
9 3H), 3.41-3.48 (m, 2 H), 6.90-6.95 (m, 1H) 7.25-7.28 (m, 1H), 8.12-8.20 (m, 1H), 8.21-8.26
10
11 (m, 1H). LC-MS (M+H) 235. The flask containing this material (811 mg, 3.46 mmol) was
12
13 charged with absolute EtOH (20 mL). The flask was evacuated and backfilled with N₂ (2x),
14
15 and then 10% palladium on carbon (115 mg, 0.11 mmol) was added. The flask was then
16
17 evacuated and backfilled with H₂ via a filled balloon (this was repeated twice), and the
18
19 resulting mixture was allowed to stir at room temperature under 1 atm H₂. After stirring
20
21 overnight, the flask was evacuated and backfilled with N₂, and the mixture was suction
22
23 filtered through a pad of Celite. The reaction flask and filter cake were washed well with
24
25 EtOH, and the combined filtrates were concentrated under reduced pressure to give the title
26
27 compound as a grey-colored oil (687 mg, 97% over 2 steps). ¹H NMR (400 MHz, DMSO-*d*₆)
28
29 δ ppm 1.21 (t, *J*=7.1 Hz, 3H), 3.01-3.11 (m, 2H), 4.66-4.75 (m, 1H), 5.19 (br. s., 2H), 6.49-
30
31 6.53 (m, 1H), 6.56-6.61 (m, 1H), 6.67-6.74 (m, 1H). LC-MS (M+H) 205.

32
33
34
35
36 **(*R*)-*tert*-Butyl (1-((2-(ethylamino)-4-(trifluoromethyl)phenyl)amino)-1-oxopropan-**
37
38 **2-yl)carbamate (50):** A 250 mL roundbottom flask containing **49** (687 mg, 3.36 mmol) was
39
40 charged with (*R*)-2-((*tert*-butoxycarbonyl)amino)propanoic acid (700 mg, 3.70 mmol) and
41
42 anhydrous DMF (14 mL). The solution was treated with triethylamine (0.52 mL, 3.73 mmol)
43
44 and was cooled to 0 °C before HATU (1.44 g, 3.79 mmol) was added. Additional DMF (1
45
46 mL) was added, and the resulting solution was allowed to stir at 0 °C with slow warming to
47
48 room temperature. After stirring overnight, the reaction mixture was partitioned between
49
50 EtOAc and water. The aqueous layer was extracted with EtOAc, and the combined organics
51
52 were concentrated under reduced pressure. The crude material was purified by silica gel
53
54 chromatography (gradient elution; *R*_f in 60:40 hexanes:EtOAc = 0.43) to give the title
55
56
57
58
59
60

1
2
3 compound as a colorless solid (968 mg, 77%). ¹H NMR (400 MHz, DMSO-*d*₆) δ ppm 1.20
4 (t, *J*=7.0 Hz, 3H), 1.27 (d, *J*=7.0 Hz, 3H), 1.39 (s, 9H), 3.07 -3.16 (m, 2H), 4.02-4.13 (m,
5 1H), 5.13-5.21 (m, 1H), 6.77-6.81 (m, 1H), 6.84-6.89 (m, 1H), 7.15-7.20 (m, 1H), 7.27-7.33
6 (m, 1H), 9.32-9.39 (m, 1H). LC-MS (M+H) 376.

7
8
9
10
11 **(*R*)-*tert*-Butyl (1-(1-ethyl-6-(trifluoromethyl)-1*H*-benzo[d]imidazol-2-
12 yl)ethyl)carbamate (51):** A 250 mL roundbottom flask containing **50** (603 mg, 1.61 mmol)
13 was charged with glacial HOAc (10 mL), and the resulting mixture was heated in a 65 °C oil
14 bath for 2 hours. The reaction was allowed to cool and was concentrated under reduced
15 pressure, and the crude material was purified by silica gel chromatography (gradient elution;
16 R_f in 60:40 hexanes:EtOAc = 0.47) to give the product as a colorless solid (491 mg, 86%).
17
18 ¹H NMR (400 MHz, DMSO-*d*₆) δ ppm 1.31 (t, *J*=7.0 Hz, 3H), 1.37 (s, 9H), 1.50 (d, *J*=7.0
19 Hz, 3H), 4.28-4.46 (m, 2H), 5.00-5.11 (m, 1H), 7.45-7.51 (m, 1H), 7.54-7.61 (m, 1H), 7.74-
20 7.80 (m, 1H), 7.96-8.02 (m, 1H). LC-MS (M+H) 358.

21
22
23 **(*R*)-4-Chloro-*N*-(1-(1-ethyl-6-(trifluoromethyl)-1*H*-benzo[d]imidazol-2-
24 yl)ethyl)benzenesulfonamide (4):** A 100 mL roundbottom flask was charged with **51** (202
25 mg, 0.57 mmol). A solution of 4 N HCl in dioxane (4.0 mL, 16 mmol) was added, and the
26 resulting solution was allowed to stir at room temperature. After 2 hours, the mixture was
27 concentrated under reduced pressure. The residue was dissolved in CH₂Cl₂ (5.0 mL), and
28 then was treated with triethylamine (250 μL, 1.79 mmol) before being cooled to 0 °C. The
29 mixture was then treated with 4-chlorobenzenesulfonyl chloride (171 mg, 0.81 mmol) and
30 was allowed to stir at 0 °C. After 2 hours, the mixture was partitioned between CH₂Cl₂ and
31 water. The aqueous layer was extracted with CH₂Cl₂, and the combined organics were
32 concentrated under reduced pressure. The crude material was purified by silica gel
33 chromatography (gradient elution; R_f in 60:40 hexanes:EtOAc = 0.33) to give the title
34 compound as a colorless solid (152 mg, 62%). ¹H NMR (400 MHz, DMSO-*d*₆) δ ppm 1.29
35
36
37
38
39
40
41
42
43
44
45
46
47
48
49
50
51
52
53
54
55
56
57
58
59
60

(t, $J=7.5$ Hz, 3H), 1.40 (t, $J=7.0$ Hz, 3H), 4.26-4.42 (m, 2H), 4.81-4.92 (m, 1H), 7.35-7.42 (m, 2H), 7.43-7.49 (m, 1H), 7.62-7.70 (m, 3H), 7.91-7.97 (m, 1H), 8.59-8.66 (m, 1H). LC-MS (M+H) 432.

The compounds described in Table 2 were prepared using procedures analogous to those described above for compound 4.

(R)-4-Chloro-N-(1-(1-ethyl-6-methoxy-1H-benzo[d]imidazol-2-yl)ethyl)benzenesulfonamide (3): ^1H NMR (300 MHz, CDCl_3) δ ppm 1.33 (t, 3H), 1.52 (d, 3H), 3.86 (s, 3H), 3.98 (m, 1H), 4.15 (m, 1H), 4.82 (m, 1H), 6.60 (m, 1H), 6.86 (m, 1H), 7.15 (m, 1H), 7.25 (m, 2H), 7.51 (m, 1H), 7.69 (m, 2H). LC-MS (M+H) 394.

(R)-4-Chloro-N-(1-(6-chloro-1-ethyl-5-fluoro-1H-benzo[d]imidazol-2-yl)ethyl)benzenesulfonamide (5): ^1H NMR (400 MHz, CDCl_3) δ ppm 1.40 (t, $J=7.5$ Hz, 3H), 1.60 ($J=6.0$ Hz, 3H), 4.01-4.13 (m, 1H), 4.14-4.26 (m, 1H), 4.75-4.85 (m, 1H), 5.81-5.89 (m, 1H), 7.22-7.30 (m, 2H), 7.31-7.35 (m, 1H), 7.37-7.42 (m, 1H), 7.61-7.68 (m, 2H). LC-MS (M+H) 417.

(R)-4-Chloro-N-(1-(5-cyano-1-ethyl-1H-benzo[d]imidazol-2-yl)ethyl)benzenesulfonamide (6): ^1H NMR (300 MHz, CDCl_3) δ ppm 1.43 (t, 3H), 1.59 (d, 3H), 4.16 (m, 1H), 4.28 (m, 1H), 4.88 (m, 1H), 6.22 (m, 1H), 7.25 (m, 2H), 7.37 (m, 1H), 7.54 (m, 1H), 7.67 (m, 2H), 7.95 (m, 1H). LC-MS (M+H) 389.

(R)-4-Chloro-N-(1-(1-ethyl-5-(hydroxymethyl)-1H-benzo[d]imidazol-2-yl)ethyl)benzenesulfonamide (7): ^1H NMR (400 MHz, $\text{DMSO}-d_6$) δ ppm 1.29 (t, $J=7.2$ Hz, 3H), 1.35 (d, $J=6.8$ Hz, 3H), 4.20-4.31 (m, 2H), 4.58 (m, 2H), 4.79-4.90 (m, 1H), 5.12 (br. s., 1H), 7.20 (m, 1H), 7.44 (m, 1H), 7.46 (m, 1H), 7.52 (m, 2H), 7.75 (m, 2H), 8.55 (m, 1H). LC-MS (M+H) 394.

(R)-4-Chloro-N-(1-(1-ethyl-6-(hydroxymethyl)-1H-benzo[d]imidazol-2-yl)ethyl)benzenesulfonamide (8): ^1H NMR (400 MHz, $\text{DMSO}-d_6$) δ ppm 1.29 (t, $J=7.1$ Hz,

1
2
3 3H), 1.33 (d, $J=6.8$ Hz, 3H), 4.24 (m, 2H), 4.60 (d, $J=5.8$ Hz, 2H), 4.82 (m, 1H), 5.18 (t,
4
5 $J=5.8$ Hz, 1H), 7.11 (m, 1H), 7.41 (m, 1H), 7.45 (m, 1H), 7.51 (m, 2H), 7.74 (m, 2H), 8.52
6
7 (m, 1H). LC-MS (M+H) 394.

8
9
10 **(R)-2-(1-(4-Chlorophenylsulfonamido)ethyl)-1-ethyl-1H-benzo[d]imidazole-5-**
11 **carboxamide (9):** ^1H NMR (300 MHz, DMSO- d_6) δ ppm 1.32 (t, $J=7.1$ Hz, 3H), 1.40 (d,
12
13 $J=6.8$ Hz, 3H), 4.35 (m, 2H), 4.86-4.97 (m, 1H), 7.34 (br. s., 1H), 7.52 (m, 2H), 7.67 (m, 1H),
14
15 7.74 (m, 2H), 7.84-7.95 (m, 1H), 8.00 (br. s., 1H), 8.12 (m, 1H), 8.72 (m, 1H). LC-MS
16
17 (M+H) 407.

18
19
20
21 **(R)-4-Chloro-N-(1-(6-((dimethylamino)methyl)-1-ethyl-1H-benzo[d]imidazol-2-**
22 **yl)ethyl)benzenesulfonamide (10):** ^1H NMR (300 MHz, DMSO- d_6) δ ppm 1.31-1.44 (m,
23
24 6H), 2.74 (m, 6H), 4.31 (m, 2H), 4.39 (m, 2H), 4.90 (m, 1H), 7.33 (m, 1H), 7.49 (m, 2H),
25
26 7.63 (m, 1H), 7.71 (m, 3H), 8.70 (m, 1H). LC-MS (M+H) 421.

27
28
29
30 **(R)-4-Chloro-N-(1-(1-ethyl-5-morpholino-1H-benzo[d]imidazol-2-**
31 **yl)ethyl)benzenesulfonamide (11):** ^1H NMR (300 MHz, DMSO- d_6) δ ppm 1.26 (t, 3H), 1.33
32
33 (d, 3H), 3.03 (m, 4H), 3.75 (m, 4H), 4.18 (m, 2H), 4.76 (m, 1H), 6.97 (m, 2H), 7.33 (m, 1H),
34
35 7.46 (m, 2H), 7.69 (m, 2H), 8.48 (m, 1H). LC-MS (M+H) 449.

36
37
38
39 **(R)-4-Chloro-N-(1-(1-ethyl-6-(methylsulfonyl)-1H-benzo[d]imidazol-2-**
40 **yl)ethyl)benzenesulfonamide (12):** ^1H NMR (300 MHz, DMSO- d_6) δ ppm 1.33 (t, $J=7.2$
41
42 Hz, 3H), 1.39 (d, $J=6.8$ Hz, 3H), 3.22 (s, 3H), 4.38 (m, 2H), 4.85-4.94 (m, 1H), 7.41 (m,
43
44 2H), 7.66 (m, 2H), 7.69 (m, 2H), 8.10 (m, 1H), 8.65 (m, 1H). LC-MS (M+H) 442.

45
46
47
48 **(R)-4-Chloro-N-(1-(7-chloro-1-ethyl-1H-benzo[d]imidazol-2-**
49 **yl)ethyl)benzenesulfonamide (13):** ^1H NMR (300 MHz, DMSO- d_6) δ ppm 1.35-1.39 (m,
50
51 6H), 4.39-4.55 (m, 2H), 4.83-4.89 (m, 1H), 7.13-7.26 (m, 2H), 7.43-7.51 (m, 3H), 7.67-7.71
52
53 (m, 2H), 8.63 (br. s., 1H). LC-MS (M+H) 399.
54
55
56
57
58
59
60

4-Chloro-*N*-(1-(3-ethyl-3*H*-imidazo[4,5-*b*]pyridin-2-yl)ethyl)benzenesulfonamide

(14): ¹H NMR (300 MHz, DMSO-*d*₆) δ ppm 1.30 (t, 3H), 1.40 (d, 3H), 4.30 (q, 2H), 4.81-4.95 (m, 1H), 7.18-7.27 (m, 1H), 7.45 (d, 2H), 7.70 (d, 2H), 7.92-8.00 (m, 1H), 8.32-8.39 (m, 1H), 8.65-8.73 (m, 1H). LC-MS (M+H) 365.

4-Chloro-*N*-(1-(3-ethyl-3*H*-imidazo[4,5-*c*]pyridin-2-yl)ethyl)benzenesulfonamide

(15): ¹H NMR (300 MHz, MeOH-*d*₄) δ ppm 1.45 (t, *J*=7.2 Hz, 3H), 1.52 (d, *J*=7.2 Hz, 3H), 4.39-4.49 (m, 2H), 4.90-5.00 (m, 1H), 7.26-7.32 (m 2H), 7.49-7.54 (m, 1H), 7.62-7.68 (m, 2H), 8.27-8.31 (m, 1H), 8.80-8.83 (m, 1H). LC-MS (M+H) 365.

4-Chloro-*N*-(1-(1-ethyl-1*H*-imidazo[4,5-*c*]pyridin-2-yl)ethyl)benzenesulfonamide

(16): ¹H NMR (300 MHz, MeOH-*d*₄) δ ppm 1.60 (t, 3H), 1.66 (d, 3H), 4.45 (q, 2H), 5.01 (m, 1H), 7.34 (m, 2H), 7.60 (m, 2H), 7.75 (m, 2H), 8.33 (m, 1H), 8.86 (m, 1 H). LC-MS (M+H) 365.

4-Chloro-*N*-(1-(1-ethyl-1*H*-imidazo[4,5-*b*]pyridin-2-yl)ethyl)benzenesulfonamide

(17): ¹H NMR (300 MHz, MeOH-*d*₄) δ ppm 1.40 (t, 3H), 1.65 (d, 3H), 4.37 (q, 2H), 4.86 (m, 1H), 7.28 (m, 2H), 7.41 (d, 2H), 7.64 (d, 2H), 7.88 (d, 1H), 8.45 (d, 1H). LC-MS (M+H) 365.

The compounds described in Tables 4 and 5 were prepared from intermediate **51** and the appropriate sulfonyl chloride, following the same procedure as that employed for compound **4**.

(*R*)-*N*-(1-(1-Ethyl-6-(trifluoromethyl)-1*H*-benzo[*d*]imidazol-2-yl)ethyl)cyclopropanesulfonamide (18): ¹H NMR (300 MHz, CDCl₃) δ ppm 0.83 (m, 1H), 0.97 (m, 1H), 1.11 (m, 1H), 1.21 (m, 1H), 1.59 (t, 3H), 1.85 (d, 3H), 2.33 (m, 1H), 4.34-4.52 (m, 2H), 5.09 (m, 1H), 6.34 (m, 1H), 7.67 (d, 1H), 7.75 (m, 1H), 7.92 (m, 1H). LC-MS (M+H) 362.

1
2
3 **(R)-N-(1-(1-Ethyl-6-(trifluoromethyl)-1H-benzo[d]imidazol-2-**
4 **yl)ethyl)cyclopentanesulfonamide (19):** ¹H NMR (300 MHz, CDCl₃) δ ppm 1.55 (m, 5H),
5 1.70-1.75 (m, 2H), 1.81 (d, 3H), 1.90-2.01 (m, 4H), 3.36 (m, 1H), 4.30-4.51 (m, 2H), 5.08
6 (m, 1H), 7.19 (m, 1H), 7.70 (m, 1H), 7.92 (m, 1H). LC-MS (M+H) 390.

7
8
9
10
11 **(R)-N-(1-(1-Ethyl-6-(trifluoromethyl)-1H-benzo[d]imidazol-2-**
12 **yl)ethyl)benzenesulfonamide (20):** ¹H NMR (300 MHz, CDCl₃) δ ppm 1.44 (t, 3H), 1.66 (d,
13 3H), 4.19 (m, 1H), 4.30 (m, 1H), 4.90 (m, 1H), 6.98 (m, 1H), 7.24-7.35 (m, 3H), 7.54-7.58
14 (m, 2H), 7.71-7.77 (m, 3H). LC-MS (M+H) 398.

15
16
17
18
19
20
21 **(R)-N-(1-(1-Ethyl-6-(trifluoromethyl)-1H-benzo[d]imidazol-2-yl)ethyl)-4-**
22 **fluorobenzenesulfonamide (21):** ¹H NMR (300 MHz, CDCl₃) δ ppm 1.39 (t, 3H), 1.54 (d,
23 3H), 4.12 (m, 1H), 4.29 (m, 1H), 4.90 (m, 1H), 6.98 (m, 2H), 7.13 (m, 1H), 7.48 (m, 2H),
24 7.78 (m, 3H). LC-MS (M+H) 416.

25
26
27
28
29
30
31 **(R)-N-(1-(1-Ethyl-6-(trifluoromethyl)-1H-benzo[d]imidazol-2-yl)ethyl)-4-**
32 **methylbenzenesulfonamide (22):** ¹H NMR (300 MHz, DMSO-*d*₆) δ ppm 1.29 (t, *J*=7.1 Hz,
33 3H), 1.35 (d, *J*=6.8 Hz, 3H), 2.21 (s, 3H), 4.28-4.40 (m, 2H), 4.82 (m, 1H), 7.17 (m, 2H),
34 7.43-7.53 (m, 1H), 7.58 (m, 2H), 7.69 (m, 1H), 7.94 (m, 1H), 8.39 (m, 1H). LC-MS (M+H)
35 412.

36
37
38
39
40
41 **(R)-4-Cyano-N-(1-(1-ethyl-6-(trifluoromethyl)-1H-benzo[d]imidazol-2-**
42 **yl)ethyl)benzenesulfonamide (23):** ¹H NMR (300 MHz, CDCl₃) δ ppm 1.43 (t, 3H), 1.58 (d,
43 3H), 4.15 (m, 1H), 4.31 (m, 1H), 4.95 (m, 1H), 7.25 (m, 1H), 7.51-7.59 (m, 4H), 7.75 (m,
44 1H), 7.87 (m, 2H). LC-MS (M+H) 423.

45
46
47
48
49
50
51 **(R)-3-Chloro-N-(1-(1-ethyl-6-(trifluoromethyl)-1H-benzo[d]imidazol-2-**
52 **yl)ethyl)benzenesulfonamide (24):** ¹H NMR (300 MHz, CDCl₃) δ ppm 1.48 (t, 3H), 1.68 (d,
53 3H), 4.14-4.40 (m, 2H), 4.91 (m, 1H), 6.27 (m, 1H), 7.20 (m, 2H), 7.55 (m, 1H), 7.60 (m,
54 1H), 7.64 (m, 2H), 7.69 (m, 1H). LC-MS (M+H) 433.

1
2
3 **(R)-3-Cyano-N-(1-(1-ethyl-6-(trifluoromethyl)-1H-benzo[d]imidazol-2-**
4 **yl)ethyl)benzenesulfonamide (25):** ¹H NMR (300 MHz, CDCl₃) δ ppm 1.46 (t, 3H), 1.65 (d,
5 3H), 4.14-4.27 (m, 1H), 4.27-4.39 (m, 1H), 4.91 (m, 1H), 6.90 (m, 1H), 7.35 (m, 1H), 7.43
6 3H), 4.14-4.27 (m, 1H), 4.27-4.39 (m, 1H), 4.91 (m, 1H), 6.90 (m, 1H), 7.35 (m, 1H), 7.43
7 (m, 1H), 7.54 (m, 1H), 7.62 (m, 2H), 7.83 (m, 1H), 7.95 (m, 1H). LC-MS (M+H) 423.
8
9

10
11 **(R)-N-(4-(N-(1-(1-Ethyl-6-(trifluoromethyl)-1H-benzo[d]imidazol-2-**
12 **yl)ethyl)sulfamoyl)-2-methylphenyl)acetamide (26):** ¹H NMR (300 MHz, CDCl₃) δ ppm
13 1.41 (t, 3H), 1.73 (d, 3H), 1.86 (s, 3H), 2.08 (s, 3H), 4.18 (m, 2H), 4.83 (m, 1H), 6.65 (m,
14 1H), 7.45-7.58 (m, 4H), 7.75 (m, 1H), 7.83 (m, 1H). LC-MS (M+H) 469.
15
16
17
18
19

20
21 **(R)-N-(1-(1-Ethyl-6-(trifluoromethyl)-1H-benzo[d]imidazol-2-yl)ethyl)-4-**
22 **isobutylbenzenesulfonamide (27):** ¹H NMR (300 MHz, CDCl₃) δ ppm 0.66 (d, 6H), 1.33 (t,
23 3H), 1.48-1.60 (m, 1H), 1.57 (d, 3H), 2.19 (d, 2H), 3.99-4.11 (m, 1H), 4.13-4.26 (m, 1H),
24 3H), 1.48-1.60 (m, 1H), 1.57 (d, 3H), 2.19 (d, 2H), 3.99-4.11 (m, 1H), 4.13-4.26 (m, 1H),
25 4.79 (m, 1H), 6.07 (m, 1H), 6.89 (m, 2H), 7.44 (s, 1H), 7.46 (s, 1H), 7.53 (m, 2H), 7.63 (m,
26 1H), 7.53 (m, 1H), 7.61 (m, 1H). LC-MS (M+H) 454.
27
28
29
30

31
32 **(R)-N-(1-(1-Ethyl-6-(trifluoromethyl)-1H-benzo[d]imidazol-2-yl)ethyl)-2,4,6-**
33 **trifluorobenzenesulfonamide (28):** ¹H NMR (300 MHz, CDCl₃) δ ppm 1.39 (t, 3H), 1.67 (d,
34 3H), 4.17 (m, 1H), 4.35 (m, 1H), 5.02 (m, 1H), 6.27 (m, 1H), 6.32-6.40 (m, 2H), 7.46 (m,
35 3H), 4.17 (m, 1H), 4.35 (m, 1H), 5.02 (m, 1H), 6.27 (m, 1H), 6.32-6.40 (m, 2H), 7.46 (m,
36 1H), 7.53 (m, 1H), 7.61 (m, 1H). LC-MS (M+H) 452.
37
38
39

40
41 **(R)-N-(1-(1-Ethyl-6-(trifluoromethyl)-1H-benzo[d]imidazol-2-yl)ethyl)pyridine-2-**
42 **sulfonamide (29):** ¹H NMR (300 MHz, CDCl₃) δ ppm 1.49 (t, 3H), 1.65 (d, 3H), 4.23 (m,
43 1H), 4.42 (m, 1H), 5.20 (m, 1H), 7.13 (m, 1H), 7.22 (m, 1H), 7.44 (m, 1H), 7.65-7.75 (m,
44 1H), 4.42 (m, 1H), 5.20 (m, 1H), 7.13 (m, 1H), 7.22 (m, 1H), 7.44 (m, 1H), 7.65-7.75 (m,
45 2H), 7.90 (m, 1H), 8.32 (m, 1H). LC-MS (M+H) 399.
46
47
48

49
50 **(R)-N-(1-(1-Ethyl-6-(trifluoromethyl)-1H-benzo[d]imidazol-2-yl)ethyl)pyridine-3-**
51 **sulfonamide (30):** ¹H NMR (300 MHz, CDCl₃) δ ppm 1.40 (t, 3H), 1.58 (d, 3H), 4.06-4.36
52 (m, 2H), 4.87-4.98 (m, 1H), 6.96-7.05 (m, 1H), 7.14-7.21 (m, 1H), 7.44-7.51 (m, 2H), 7.68-
53 (m, 2H), 4.87-4.98 (m, 1H), 6.96-7.05 (m, 1H), 7.14-7.21 (m, 1H), 7.44-7.51 (m, 2H), 7.68-
54 7.74 (m, 1H), 7.96-8.02 (m, 1H), 8.51-8.55 (m, 1H), 8.98-9.02 (m, 1H). LC-MS (M+H) 399.
55
56
57
58
59
60

1
2
3 **(R)-N-(1-(1-Ethyl-6-(trifluoromethyl)-1H-benzo[d]imidazol-2-yl)ethyl)pyridine-4-**
4 **sulfonamide (31):** ¹H NMR (300 MHz, CDCl₃) δ ppm 1.41 (t, 3H), 1.57 (d, 3H), 1.86-1.95
5 (m, 1H), 4.07-4.36 (m, 2H), 4.93 (d, 1H), 7.46-7.54 (m, 2H), 7.59 (m, 2H), 7.68-7.74 (m,
6 1H), 8.63 (m, 2H). LC-MS (M+H) 399.

7
8
9
10
11 **(R)-N-(1-(1-Ethyl-6-(trifluoromethyl)-1H-benzo[d]imidazol-2-yl)ethyl)-1,3-**
12 **dimethyl-1H-pyrazole-4-sulfonamide (32):** ¹H NMR (300 MHz, CDCl₃) δ ppm 1.29 (s,
13 3H), 1.31 (s, 3H), 1.51 (t, 3H), 1.77 (d, 3H), 4.32 (m, 1H), 4.43 (m, 1H), 5.01 (m, 1H), 6.67
14 (m, 1H), 7.62 (m, 1H), 7.69 (m, 1H), 7.89 (m, 1H). LC-MS (M+H) 416.

15
16
17
18
19
20
21 **(R)-N-(1-(1-Ethyl-6-(trifluoromethyl)-1H-benzo[d]imidazol-2-yl)ethyl)-3-methyl-1-**
22 **propyl-1H-pyrazole-4-sulfonamide (33):** ¹H NMR (300 MHz, CDCl₃) δ ppm 0.81 (t, 3H),
23 1.51 (t, 3H), 1.66 (m, 2H), 1.73 (m, 3H), 2.39 (s, 3H), 3.77 (t, 2H), 4.30 (m, 1H), 4.38 (m,
24 1H), 4.95 (m, 1H), 6.28 (m, 1H), 7.63 (m, 2H), 7.67 (m, 1H), 7.87 (m, 1H). LC-MS (M+H)
25 444.

26
27
28
29
30
31
32 **(R)-1-Ethyl-N-(1-(1-ethyl-6-(trifluoromethyl)-1H-benzo[d]imidazol-2-yl)ethyl)-1H-**
33 **pyrazole-4-sulfonamide (34):** ¹H NMR (300 MHz, CDCl₃) δ ppm 1.21 (t, 3H), 1.50 (t, 3H),
34 1.74 (d, 3H), 3.84 (q, 2H), 4.22-4.40 (m, 2H), 4.97 (m, 1H), 6.65 (m, 1H), 7.59 (m, 1H), 7.61
35 (m, 1H), 7.63 (m, 1H), 7.71 (m, 1H), 7.86 (1, H). LC-MS (M+H) 416.

36
37
38
39
40
41 **(R)-1-Ethyl-N-(1-(1-ethyl-6-(trifluoromethyl)-1H-benzo[d]imidazol-2-yl)ethyl)-5-**
42 **methyl-1H-pyrazole-4-sulfonamide (35):** ¹H NMR (300 MHz, CDCl₃) δ ppm 1.22 (t, 3H),
43 1.67 (t, 3H), 1.90 (d, 3H), 2.57 (s, 3H), 3.90 (m, 2H), 4.45 (m, 1H), 4.59 (m, 1H), 5.12 (m,
44 1H), 7.40 (m, 1H), 7.80-7.84 (m, 3H), 7.98 (m, 1H). LC-MS (M+H) 430.

45
46
47
48
49
50 **(R)-N-(1-(1-Ethyl-6-(trifluoromethyl)-1H-benzo[d]imidazol-2-yl)ethyl)-5-methyl-1-**
51 **propyl-1H-pyrazole-4-sulfonamide (36):** ¹H NMR (300 MHz, CDCl₃) δ ppm 0.58 (t, 3H),
52 1.27 (m, 2H), 1.37 (t, 3H), 1.60 (d, 3H), 2.28 (s, 3H), 3.49 (m, 2H), 4.16 (m, 2H), 4.75 (m,
53 1H), 6.17 (m, 1H), 7.49-7.53 (m, 3H), 7.71 (m, 1H). LC-MS (M+H) 444.

1
2
3
4
5
6
7
8
9
10
11
12
13
(R)-N-(1-(1-Ethyl-6-(trifluoromethyl)-1H-benzo[d]imidazol-2-yl)ethyl)-1-isopropyl-5-methyl-1H-pyrazole-4-sulfonamide (37): ¹H NMR (300 MHz, CDCl₃) δ ppm 0.80 (d, 3H), 1.19 (d, 3H), 1.40 (t, 3H), 1.62 (d, 3H), 2.31 (s, 3H), 3.96-4.04 (m, 1H), 4.09-4.31 (m, 2H), 4.80 (m, 1H), 6.38 (m, 1H), 7.46 (m, 1H), 7.51 (m, 1H), 7.55 (m, 1H), 7.70 (m, 1H). LC-MS (M+H) 444.

14
15
16
17
18
19
20
21
22
(R)-N-(1-(1-Ethyl-6-(trifluoromethyl)-1H-benzo[d]imidazol-2-yl)ethyl)-1,2-dimethyl-1H-imidazole-4-sulfonamide (38): ¹H NMR (300 MHz, CDCl₃) δ ppm 1.42 (t, 3H), 1.65 (d, 3H), 1.85 (s, 3H), 3.60 (s, 3H), 4.18 (m, 2H), 4.76 (m, 1H), 6.57 (m, 1H), 7.41 (m, 1H), 7.54 (m, 1H), 7.60 (m, 1H), 7.78 (m, 1H). LC-MS (M+H) 416.

23
24
25
26
27
28
29
30
31
(R)-N-(1-(1-Ethyl-6-(trifluoromethyl)-1H-benzo[d]imidazol-2-yl)ethyl)-1,2-dimethyl-1H-imidazole-5-sulfonamide (39): ¹H NMR (300 MHz, CDCl₃) δ ppm 1.58 (t, 3H), 1.80 (d, 3H), 2.39 (s, 3H), 3.67 (s, 3H), 4.35-4.51 (m, 2H), 5.05 (m, 1H), 7.71-7.76 (m, 3H), 7.94 (m, 1H). LC-MS (M+H) 416.

32
33
34
35
36
37
38
39
40
(R)-N-(5-(N-(1-(1-Ethyl-6-(trifluoromethyl)-1H-benzo[d]imidazol-2-yl)ethyl)sulfamoyl)thiazol-2-yl)acetamide (40): ¹H NMR (300 MHz, CDCl₃) δ ppm 1.55 (t, 3H), 1.74 (d, 3H), 2.12 (s, 3H), 4.38 (m, 2H), 5.09 (m, 1H), 7.59-7.67 (m, 2H), 7.77 (m, 2H). LC-MS (M+H) 462.

41
42
43
44
45
46
47
48
49
50
51
52
53
54
55
56
57
58
59
60
2,4-Dichloro-5-nitropyridine (52): Anhydrous THF (50 mL) was cooled to -78 °C, and NH₃ (gas, about 30 mL) was condensed into the THF. Potassium *tert*-butoxide (9.3 g, 79 mmol) was added, and the mixture was allowed to warm to -35 °C. In a separate flask, 4-chloro-3-nitropyridine (4.1 g, 26 mmol) was dissolved in anhydrous THF (40 mL), and the solution was cooled to 0 °C before *tert*-butylhydroperoxide (5 M in decane; 7.0 mL, 35 mmol) was added. The resulting solution was added dropwise to the solution of potassium *tert*-butoxide mixture over 30 minutes. The resulting mixture was allowed to stir at -35 °C for an additional 30 minutes, and was then cooled to -78 °C before slowly quenching with

1
2
3 saturated NH₄Cl solution (20 mL). The mixture was allowed to warm to room temperature
4
5 open to the atmosphere overnight, and was then concentrated to small volume under reduced
6
7 pressure. The resulting suspension was filtered, and the solid was washed with cold water
8
9 (3x10 mL) and dried *in vacuo* to afford 4-chloro-5-nitropyridin-2-ol as a yellow solid (2.7 g,
10
11 60%). ¹H NMR (300 MHz, DMSO-*d*₆) δ ppm 5.95 (s, 1H), 8.80 (s, 1H). LC-MS (M-H) 173.
12
13 This material was suspended in toluene (60 mL), and POCl₃ (14.2 mL, 156 mmol) was
14
15 added. The mixture was heated at reflux for 6 h and was then heated at 60 °C overnight.
16
17 Upon cooling, the mixture was concentrated under reduced pressure. The residue was
18
19 partitioned between EtOAc and saturated K₂CO₃, and the organic layer was dried (Na₂SO₄),
20
21 filtered through a short pad of silica gel (eluting with 1:1 hexanes:EtOAc), and concentrated
22
23 under reduced pressure to give the title compound as a brown solid (2.2 g, 75%). ¹H NMR
24
25 (300 MHz, DMSO-*d*₆) δ ppm 8.23 (s, 1H), 9.18 (s, 1H). LC-MS (M-H) 193.
26
27
28

29
30 **2-Chloro-N-ethyl-5-nitropyridin-4-amine (53):** A solution of **52** (1.7 g, 8.8 mmol) in
31
32 THF (10 mL) was cooled to 0 °C, and then ethylamine (2 M solution in THF; 10 mL, 20
33
34 mmol) was slowly added. Upon completion of the reaction (as judged by TLC), the mixture
35
36 was concentrated under reduced pressure. The residue was partitioned between EtOAc and
37
38 water, and the organic layer was concentrated to give the title compound as a yellow solid
39
40 (1.44 g, 81%). ¹H NMR (300 MHz, DMSO-*d*₆) δ ppm 1.17 (m, 3H), 3.44 (m, 2H), 7.10 (s,
41
42 1H), 8.51 (s, 1H), 8.87 (s, 1H). LC-MS (M-H) 202.
43
44

45
46 **N-Ethyl-2-methoxy-5-nitropyridin-4-amine (54):** A 250 mL roundbottom flask
47
48 containing **53** (986 mg, 4.89 mmol) was charged with MeOH (25 mL) and NaOMe (1.12 g,
49
50 20.7 mmol). The mixture was heated overnight in a 65 °C oil bath, and then allowed to cool
51
52 and was concentrated under reduced pressure. The residue was partitioned between EtOAc
53
54 and water, and the aqueous layer was further extracted with EtOAc. The combined organics
55
56 were washed with brine, dried (MgSO₄), filtered, and concentrated to give the product as a
57
58
59
60

1
2
3 pale yellow solid (827 mg, 86%). ¹H NMR (300 MHz, CDCl₃) δ ppm 1.37 (t, *J*=7.2 Hz, 3H),
4
5 3.26-3.35 (m, 2H), 3.99 (s, 3H), 5.95 (s, 1H), 7.90 (br. s., 1H), 9.01 (s, 1H). LC-MS (M+H)
6
7 198.

9
10 ***N*4-Ethyl-6-methoxypyridine-3,4-diamine (55)**: A 250 mL roundbottom flask
11
12 containing **54** (827 mg, 4.19 mmol) was charged with tin (II) chloride dihydrate (3.82 g, 16.9
13
14 mmol) and EtOAc (15 mL). The resulting mixture was heated to 80 °C. After 4 hours, the
15
16 mixture was allowed to cool and was treated with aqueous NaHCO₃, precipitating a colorless
17
18 solid. The mixture was suction filtered through a pad of diatomaceous earth, and the reaction
19
20 flask and filter were thoroughly washed with water and EtOAc. The filtrate layers were
21
22 separated, and the aqueous layer was further extracted with EtOAc. The combined organics
23
24 were washed with brine, dried (MgSO₄), filtered, and concentrated to give the product as a
25
26 dark red solid (465 mg, 66%). ¹H NMR (300 MHz, CDCl₃) δ ppm 1.30 (t, *J*=7.2 Hz, 3H),
27
28 2.77 (br. s., 2H), 3.11-3.22 (m, 2H), 3.86 (s, 3H), 4.34 (br. s., 1H), 5.90 (s, 1H), 7.50 (s, 1H).
29
30 LC-MS (M+H) 168.
31
32

33
34 ***2*-Cyclopropyl-*N*-ethyl-5-nitropyridin-4-amine (56)**: A 100 mL roundbottom flask
35
36 was charged with **53** (0.60 g, 2.9 mmol), cyclopropylboronic acid (0.65 g, 7.5 mmol), and
37
38 K₃PO₄ (1.92 g, 15.0 mmol). Toluene (45 mL) and water (5 mL) were added, and N₂ was
39
40 bubbled into the mixture for 20 minutes before Pd(PPh₃)₄ (0.85 g, 0.75 mmol) was added.
41
42 The reaction was heated at 100 °C overnight, and was then allowed to cool. The mixture was
43
44 partitioned between EtOAc and water, and the aqueous layer was further extracted with
45
46 EtOAc. The combined organics were concentrated under reduced pressure, and the crude
47
48 material was purified by silica gel chromatography (0-80% EtOAc:hexane gradient) to give
49
50 the title compound as a solid (270 mg, 45%). ¹H NMR (300 MHz, DMSO-*d*₆) δ ppm 0.97
51
52 (m, 4H), 1.21 (t, *J*=7.2 Hz, 3H), 2.10 (m, 1H), 3.43 (m, 2H), 6.92 (s, 1H), 8.30 (m, 1H), 8.90
53
54 (s, 1H). LC-MS (M+H) 208.
55
56
57
58
59
60

1
2
3 **6-Cyclopropyl-N4-ethylpyridine-3,4-diamine (57)**: A mixture of **56** (0.50 g, 2.4
4 mmol) and 5% Pd/C (100 mg) in MeOH (50 mL) was stirred under 5 bar H₂ at room
5 temperature. After 3 hours, the mixture was filtered through Celite, and filter pad was
6 washed with MeOH. Concentration of the filtrate afforded the title compound as a purple
7 solid (380 mg, 89%). ¹H NMR (300 MHz, DMSO-*d*₆) δ ppm 0.72 (m, 2H), 0.75 (m, 2H),
8 1.20 (t, *J*=7.2 Hz, 3H), 1.82 (m, 1H), 3.13 (m, 2H), 4.43 (s, 2H), 5.40 (s, 1H), 6.25 (s, 1H),
9 7.46 (s, 1H). LC-MS (M+H) 178.

10
11
12 **5-Bromo-4-iodo-2-(trifluoromethyl)pyridine (58)**: A solution of 5-bromo-2-
13 (trifluoromethyl)pyridine (4.06 g, 18.0 mmol) in THF (25 mL) was dropwise added to a
14 solution of lithium diisopropylamide (9.0 mL, 18.0 mmol) in THF/heptane/ethylbenzene over
15 15 minutes at -78 °C under N₂. After 2 hours at -78 °C, a solution of iodine (4.65 g, 18.3
16 mmol) in THF (25 mL) was added dropwise over 20 minutes. The mixture was held at -78
17 °C for 15 minutes and was then poured into a mixture of 2 M Na₂S₂O₃ (10 mL) and diethyl
18 ether (20 mL). The layers were separated, and the aqueous layer was further extracted with
19 ether. The combined organics were washed with brine, dried (Na₂SO₄), filtered, and
20 concentrated under reduced pressure to give the crude product (5.08 g, 80%). This was used
21 directly without further purification. ¹H NMR (300 MHz, CDCl₃) δ ppm 7.56 (s, 1H), 8.99
22 (s, 1H). LC-MS (M+H) 352.

23
24 **5-Bromo-N-ethyl-2-(trifluoromethyl)pyridin-4-amine (59)**: A 250 mL roundbottom
25 flask was charged with **58** (4.52 g, 12.8 mmol) and EtOH (25 mL). Ethylamine (70% in
26 water; 4.0 mL, 50 mmol) was added, and the resulting suspension was placed in an 80 °C oil
27 bath. After heating overnight, additional ethylamine (4.0 mL, 50 mmol) was added, and
28 heating was continued. After an additional 24 hours, the reaction was allowed to cool and
29 was concentrated under reduced pressure. The residue was partitioned between EtOAc and
30 water, and the aqueous layer was extracted with EtOAc. The combined organics were
31
32
33
34
35
36
37
38
39
40
41
42
43
44
45
46
47
48
49
50
51
52
53
54
55
56
57
58
59
60

1
2
3 concentrated and the residue was purified by silica gel chromatography (gradient elution; R_f
4 in 95:5 hexanes:EtOAc = 0.22) to give the product as a colorless solid (2.21 g, 64%). ^1H
5 NMR (300 MHz, CDCl_3) δ ppm 1.37 (t, $J=7.2$ Hz, 3H), 3.27-3.40 (m, 2H), 5.01 (br. s., 2H),
6 6.82 (s, 1H), 8.44 (s, 1H). LC-MS (M+H) 270.

7
8
9
10
11 ***N*4-Ethyl-6-(trifluoromethyl)pyridine-3,4-diamine (60)**: An oven-dried sealable tube
12 equipped with magnetic stir bar and rubber septum was cooled under N_2 . The tube was
13 charged with $\text{Pd}_2(\text{dba})_3$ (5.55 g, 6.1 mmol), *rac*-BINAP (7.55 g, 12.1 mmol) and anhydrous
14 toluene (200 mL). The mixture was degassed, the rubber septum was replaced with a Teflon
15 screw cap, and the mixture was heated at 110 °C in an oil bath for 30 minutes. The solution
16 was then allowed to cool to room temperature, and benzophenone imine (6.61 mL, 39.5
17 mmol), **59** (8.16 g, 30.3 mmol) dissolved in toluene (100 mL), and sodium *tert*-butoxide (3.8
18 g, 39.5 mmol) were added. The mixture was degassed, the rubber septum was replaced with
19 Teflon cap, and the mixture was heated at 110 °C for 16 hours. The solution was then
20 allowed to cool to room temperature, was diluted with ether, filtered through a pad of Celite,
21 and concentrated under reduced pressure to give the imine adduct as a dark green oil. This
22 was dissolved in THF (240 mL) and the solution was treated with 2 M HCl (80 mL), and the
23 resulting mixture was allowed to stir at room temperature for 20 hours. The volatile
24 components were evaporated under reduced pressure, and the residue was partitioned
25 between EtOAc and 2 M HCl. The aqueous layer was cooled to 0 °C and was basified with
26 NaOH to pH 14. This mixture was extracted with EtOAc (2x), and the combined organics
27 were washed with brine, dried (Na_2SO_4), filtered, and concentrated to give the title compound
28 as a colorless solid (4.09 g, 64%). ^1H NMR (300 MHz, $\text{DMSO-}d_6$) δ ppm 1.21 (t, $J=7.2$ Hz,
29 3H), 3.12-3.21 (m, 2H), 5.23 (br. s., 1H), 5.65 (m, 1H), 6.65 (s, 1H), 7.69 (s, 1H). LC-MS
30 (M+H) 206.

1
2
3 **(R)-tert-Butyl 1-(4-(ethylamino)-6-methoxypyridin-3-ylamino)-1-oxopropan-2-**
4 **ylcarbamate (61):** A 250 mL roundbottom flask was charged with Boc-D-Ala-OH (1.56 g,
5 8.24 mmol) and CDI (1.34 g, 8.26 mmol). CH₂Cl₂ (20 mL) was added (gas evolution
6 observed), and the resulting solution was allowed to stir at room temperature. After 30
7 minutes, **55** (1.05 g, 6.28 mmol) was added, and the resulting solution was allowed to stir at
8 room temperature. After 90 minutes, the reaction was concentrated under reduced pressure,
9 and the residue was purified by silica gel chromatography (gradient elution; R_f in 20:80
10 hexanes:EtOAc = 0.21) to give the product as a light purple-colored foam (1.73 g, 62%).
11 Chiral LC analysis indicated >98% ee. ¹H NMR (400 MHz, DMSO-*d*₆) δ ppm 1.14 (t, *J*=7.1
12 Hz, 3H), 1.24 (d, *J*=7.1 Hz, 3H), 1.39 (s, 9H), 3.01-3.13 (m, 2H), 3.73 (s, 3H), 3.94-4.03 (m,
13 1H), 5.49-5.55 (m, 1H), 5.84 (s, 1H), 7.20-7.25 (m, 1H), 7.48 (s, 1H), 9.11 (s, 1H). LC-MS
14 (M+H) 339.

15
16
17
18
19
20
21
22
23
24
25
26
27
28
29
30 **(R)-1-(1-Ethyl-6-methoxy-1*H*-imidazo[4,5-*c*]pyridin-2-yl)ethanamine (62):** A 250
31 mL round bottom flask containing **61** (1.46 g, 4.31 mmol) was charged with 4 N HCl/dioxane
32 (15 mL), and the resulting mixture was allowed to stir at room temperature. After 2 hours, the
33 dioxane and excess HCl were evaporated under reduced pressure. The residue was dissolved
34 in absolute EtOH (15 mL), and then a solution of NaOH (726 mg, 18.2 mmol) in water (3
35 mL) was added. The mixture was heated in an 80 °C oil bath for 5.5 hours, and was then
36 allowed to cool to room temperature. The mixture was concentrated under reduced pressure,
37 and the residue was partitioned between CH₂Cl₂ and a minimum volume of water. The
38 aqueous layer was extracted with CH₂Cl₂, and the combined organics were washed with
39 brine, dried (MgSO₄), filtered, and concentrated to give the cyclized product as a dark purple
40 oil. Conversion of a portion of this material to the Boc-protected intermediate allowed for
41 determination of chirality; the compound was shown to have 80% ee, suggesting partial
42
43
44
45
46
47
48
49
50
51
52
53
54
55
56
57
58
59
60

1
2
3 epimerization of the chiral center occurs during the cyclization. This material was used
4
5 directly without further purification. LC-MS (M+H) 221.
6

7 **(R)-4-Cyano-N-(1-(1-ethyl-1*H*-imidazo[4,5-*c*]pyridin-2-
8
9 *yl*)ethyl)benzenesulfonamide (41):** ¹H NMR (300 MHz, DMSO-*d*₆) δ ppm 1.31 (t, 3H), 1.44
10
11 (d, 3H), 4.31 (m, 2H), 4.98 (m, 1H), 7.60 (m, 1H), 7.85 (m, 2H), 8.30 (m, 2H), 8.80 (m, 1H),
12
13 8.91 (m, 1H). LC-MS (M+H) 356.
14

15 **(R)-4-Cyano-N-(1-(1-ethyl-6-methoxy-1*H*-imidazo[4,5-*c*]pyridin-2-
16
17 *yl*)ethyl)benzenesulfonamide (42):** ¹H NMR (300 MHz, DMSO-*d*₆) δ ppm 1.25 (t, *J*=7.2
18
19 Hz, 3H), 1.37 (d, *J*=6.8 Hz, 3H), 3.87 (s, 3H), 4.17 (m, 2H), 4.81-4.90 (m, 1H), 6.84 (m, 1H),
20
21 7.79-7.87 (m, 4H), 8.36 (m, 1H), 8.83 (m, 1H). LC-MS (M+H) 386.
22

23 **(R)-4-Cyano-N-(1-(1-ethyl-6-(trifluoromethyl)-1*H*-imidazo[4,5-*c*]pyridin-2-
24
25 *yl*)ethyl)benzenesulfonamide (43):** ¹H NMR (300 MHz, DMSO-*d*₆) δ ppm 1.31 (t, *J*=7.1
26
27 Hz, 3H), 1.42 (d, *J*=6.8 Hz, 3H), 4.33-4.45 (m, 2H), 4.98 (m, 1H), 7.75-7.85 (m, 4H), 8.20
28
29 (m, 1H), 8.90 (m, 1H), 8.97 (m, 1H). LC-MS (M+H) 424.
30
31

32 **(R)-4-Cyano-N-(1-(6-cyclopropyl-1-ethyl-1*H*-imidazo[4,5-*c*]pyridin-2-
33
34 *yl*)ethyl)benzenesulfonamide (44):** ¹H NMR (300 MHz, DMSO-*d*₆) δ ppm 0.87-0.99 (m,
35
36 4H), 1.30 (t, *J*=7.2 Hz, 3H), 1.38 (d, *J*=6.9 Hz, 3H), 2.07-2.24 (m, 1H), 4.19-4.28 (m, 2H),
37
38 4.83-4.96 (m, 1H), 7.41 (m, 1H), 7.80-7.88 (m, 4H), 8.58 (m, 1H), 8.86 (m, 1H). LC-MS
39
40 (M+H) 396.
41
42

43
44 **6-Cyanopyridine-3-sulfonyl chloride (63):** A 500 mL roundbottom flask was charged with
45
46 water (90 mL) and was cooled to 0 °C. Thionyl chloride (17.0 mL, 233 mmol) was added
47
48 dropwise via addition funnel over 2 hours. The resulting solution was allowed to slowly
49
50 warm to room temperature overnight. After stirring overnight, CuCl (66 mg, 0.67 mmol) was
51
52 added, forming a yellow-colored solution. This was cooled to 0 °C. Meanwhile, a separate
53
54 250 mL roundbottom flask was charged with 5-aminopicolinonitrile (4.99 g, 41.89 mmol)
55
56
57
58
59
60

1
2
3 and concentrated HCl (50 mL). The solution was cooled to -5 °C, and then a solution of
4
5 sodium nitrite (4.11 g, 59.6 mmol) in water (25 mL) was added dropwise over 20 minutes.
6
7 The resulting mixture was allowed to stir at -5 °C for another 15 minutes and was then added
8
9 in small portions to the chilled aqueous sulfur dioxide solution over 30 minutes (gas
10
11 evolution occurs). The resulting mixture was allowed to stir at 0 °C for an additional hour,
12
13 and was then suction filtered. The filter cake was washed well with cold water, and was
14
15 dried in air and then *in vacuo* to give the product as a tan solid (5.52 g, 65%). ¹H NMR (300
16
17 MHz, CDCl₃) δ ppm 7.95-7.99 (m, 1H), 8.45-8.52 (m, 1H), 9.32 (s, 1H).
18
19

20
21 **(R)-6-Cyano-N-(1-(1-ethyl-6-methoxy-1H-imidazo[4,5-c]pyridin-2-**
22
23 **yl)ethyl)pyridine-3-sulfonamide (45):** ¹H NMR (300 MHz, DMSO-*d*₆) δ ppm 1.25 (t, *J*=7.2
24
25 Hz, 3H), 1.43 (d, *J*=6.8 Hz, 3H), 3.87 (s, 3H), 4.18 (m, 2H), 4.92 (m, 1H), 6.85 (m, 1H), 7.98
26
27 (m, 1H), 8.18 (m, 1H), 8.30 (m, 1H), 8.86 (m, 1H), 9.11 (m, 1H). LC-MS (M+H) 387.
28
29

30
31 **(R)-6-Cyano-N-(1-(1-ethyl-6-(trifluoromethyl)-1H-imidazo[4,5-c]pyridin-2-**
32
33 **yl)ethyl)pyridine-3-sulfonamide (46):** ¹H NMR (300 MHz, DMSO-*d*₆) δ ppm 1.32 (t, *J*=7.1
34
35 Hz, 3H), 1.46 (d, *J*=6.8 Hz, 3H), 4.36-4.46 (m, 2H), 5.05 (m, 1H), 8.00 (m, 1H), 8.18-8.24
36
37 (m, 2H), 8.87 (m, 2H), 9.25 (m, 1H). LC-MS (M+H) 425.
38
39

40
41 **(R)-6-Cyano-N-(1-(6-cyclopropyl-1-ethyl-1H-imidazo[4,5-c]pyridin-2-**
42
43 **yl)ethyl)pyridine-3-sulfonamide (47):** ¹H NMR (300 MHz, DMSO-*d*₆) δ ppm 0.89-0.98 (m,
44
45 4H), 1.30 (t, *J*=7.0 Hz, 3H), 1.44 (d, *J*=6.9 Hz, 3H), 2.03-2.28 (m, 1H), 4.25 (m, 2H), 4.95
46
47 (m, 1H), 7.42 (m, 1H), 7.95 (m, 1H), 8.17 (m, 1H), 8.51 (m, 1H), 8.85 (m, 1H), 9.14 (m, 1H).
48
49 LC-MS (M+H) 397.
50
51

52 Associated Content

53
54 **Supporting Information Available:** Protocols for physical property, ADMET, and
55
56 pharmacokinetic assays described in this paper, characterization of mode of inhibition for
57
58
59
60

1
2
3 compound **2**, protocol for S1P₁ receptor internalization assay, procedures for Matrigel plug
4
5 angiogenesis and Evans blue dye pharmacodynamic experiments along with accompanying
6
7 pharmacokinetic data and photographs, pharmacokinetic data from Calu6 tumor xenograft
8
9 studies, and crystallographic collection and refinement data for PXR-compound **4** complex.
10
11 This material is available free of charge via the Internet at <http://pubs.acs.org>.
12
13

14 *PDB ID Codes*

15
16 Coordinates for the structure of compound **4** bound to human PXR have been deposited in the
17
18 Protein Data Bank (PDB) under accession code 5A86.
19

20 *Author Information*

21 Corresponding Author

22 *Phone: (781) 839-4153. E-mail: edward.hennessy@astrazeneca.com

23 Notes

24 The authors declare no competing financial interest.
25
26
27
28

29 *Acknowledgments*

30
31 We are grateful to Erika Keeton, Meghan Scarpitti, Vicki Racicot, and Mali Wold for
32
33 conducting the S1P₁ translocation assay, to Nancy DeGrace and Kanayo Azogu for analytical
34
35 chemistry support, to Adrian Fretland and Helen Rollison for helpful discussions around
36
37 CYP3A induction and PXR activation, to Karen Stams, Suzette Haney, and Dave Ayres for
38
39 human hepatocyte induction studies, and to Frank Kilty for assistance in data analysis.
40
41
42

43 *Abbreviations Used*

44
45 S1P, sphingosine 1-phosphate; S1P₁, sphingosine 1-phosphate receptor 1; GIRK, G protein-
46
47 coupled inwardly rectifying potassium channel; LLE, lipophilic ligand efficiency; F%, oral
48
49 bioavailability; CL_{int}, intrinsic clearance; PXR, pregnane X receptor; CAR, constitutive
50
51 androstane receptor; FGF, fibroblast growth factor; HPMC, hydroxypropyl methylcellulose;
52
53 EBD, Evans blue dye; HATU, (dimethylamino)-*N,N*-dimethyl(3*H*-[1,2,3]triazolo[4,5-

1
2
3 *b*]pyridin-3-yloxy)methaniminium hexafluorophosphate; LDA, lithium diisopropylamide;
4
5 CDI, 1,1'-carbonyldiimidazole.
6
7
8

9 10 **References**

- 11
12 (1) Brinkmann, V. Sphingosine 1-phosphate receptors in health and disease: Mechanistic
13
14 insights from gene deletion studies and reverse pharmacology. *Pharmacol. Ther.* **2007**, *115*,
15
16 84-105.
17
18 (2) Adachi, K.; Kohara, T.; Nakao, N.; Arita, M.; Chiba, K.; Mishina, T.; Sasaki, S.; Fujita,
19
20 T. Design, Synthesis, and Structure-Activity Relationships of 2-Substituted-2-Amino-1,3-
21
22 Propanediols: Discovery of a Novel Immunosuppressant, FTY720. *Bioorg. Med. Chem. Lett.*
23
24 **1995**, *5*, 853-856.
25
26 (3) Brinkmann, V.; Davis, M. D.; Heise, C. E.; Albert, R.; Cottens, S.; Hof, R.; Bruns, C.;
27
28 Prieschl, E.; Baumruker, T.; Hiestand, P.; Foster, C. A.; Zollinger, M.; Lynch, K. R. The
29
30 Immune Modulator FTY720 Targets Sphingosine 1-Phosphate Receptors. *J. Biol. Chem.*
31
32 **2002**, *277*, 21453-21457.
33
34 (4) Mandala, S.; Hajdu, R.; Bergstrom, J.; Quackenbush, E.; Xie, J.; Milligan, J.; Thornton,
35
36 R.; Shei, G.-J.; Card, D.; Keohane, C.; Rosenbach, M.; Hale, J.; Lynch, C. L.; Rupprecht, K.;
37
38 Parsons, W.; Rosen, H. Alteration of Lymphocyte Trafficking by Sphingosine-1-Phosphate
39
40 Receptor Agonists. *Science* **2002**, *296*, 346-349.
41
42 (5) Brinkmann, V.; Billich, A.; Baumruker, T.; Heining, P.; Schmouder, R.; Francis, G.;
43
44 Aradhye, S.; Burtin, P. Fingolimod (FTY720): discovery and development of an oral drug to
45
46 treat multiple sclerosis. *Nat. Rev. Drug Disc.* **2010**, *9*, 883-897.
47
48 (6) Gräler, M. H.; Goetzl, E. J. The immunosuppressant FTY720 down-regulates
49
50 sphingosine 1-phosphate G-protein-coupled receptors. *FASEB J.* **2004**, *18*, 551-553.
51
52
53
54
55
56
57
58
59
60

1
2
3 (7) Gonzalez-Cabrera, P. J.; Hla, T.; Rosen, H. Mapping Pathways Downstream of
4 Sphingosine 1-Phosphate Subtype 1 by Differential Chemical Perturbation and Proteomics. *J.*
5 *Biol. Chem.* **2007**, *282*, 7254-7264.
6
7

8
9 (8) Oo, M. L.; Thangada, S.; Wu, M.-T.; Liu, C. H.; Macdonald, T. L.; Lynch, K. R.; Lin, C.-
10 Y.; Hla, T. Immunosuppressive and Anti-angiogenic Sphingosine 1-Phosphate Receptor-1
11 Agonists Induce Ubiquitinylation and Proteasomal Degradation of the Receptor. *J. Biol.*
12 *Chem.* **2007**, *282*, 9082-9089.
13
14

15
16 (9) Liu, Y.; Wada, R.; Yamashita, T.; Mi, Y.; Deng, C.-X.; Hobson, J. P.; Rosenfeldt, H. M.;
17 Nava, V. E.; Chae, S.-S.; Lee, M.-J.; Liu, C. H.; Hla, T.; Spiegel, S.; Proia, R. L. Edg-1, the
18 G protein-coupled receptor for sphingosine-1-phosphate, is essential for vascular maturation.
19 *J. Clin. Invest.* **2000**, *106*, 951-961.
20
21

22
23 (10) Chae, S.-S.; Paik, J.-H.; Furneaux, H.; Hla, T. Requirement for sphingosine 1-phosphate
24 receptor-1 in tumor angiogenesis demonstrated by in vivo RNA interference. *J. Clin. Invest.*
25 **2004**, *114*, 1082-1089.
26
27

28
29 (11) LaMontagne, K.; Littlewood-Evans, A.; Schnell, C.; O'Reilly, T.; Wyder, L.; Sanchez,
30 T.; Probst, B.; Butler, J.; Wood, A.; Liau, G.; Billy, E.; Theuer, A.; Hla, T.; Wood, J.
31 Antagonism of Sphingosine-1-Phosphate Receptors by FTY720 Inhibits Angiogenesis and
32 Tumor Vascularization. *Cancer Res.* **2006**, *66*, 221-231.
33
34

35
36 (12) Budde, K.; Schmouder, R. L.; Brunkhorst, R.; Nashan, B.; Lücker, P. W.; Mayer, T.;
37 Choudhury, S.; Skerjanec, A.; Kraus, G.; Neumayer, H. H. First Human Trial of FTY720, a
38 Novel Immunomodulator, in Stable Renal Transplant Patients. *J. Am. Soc. Nephrol.* **2002**, *13*,
39 1073-1083.
40
41

42
43 (13) Forrest, M.; Sun, S.-Y.; Hajdu, R.; Bergstrom, J.; Card, D.; Doherty, G.; Hale, J.;
44 Keohane, C.; Meyers, C.; Milligan, J.; Mills, S.; Nomura, N.; Rosen, H.; Rosenbach, M.;
45 Shei, G.-J.; Singer, I. I.; Tian, M.; West, S.; White, V.; Xie, J.; Proia, R. L.; Mandala, S.
46
47
48
49
50
51
52
53
54
55
56
57
58
59
60

1
2
3 Immune Cell Regulation and Cardiovascular Effects of Sphingosine 1-Phosphate Receptor
4 Agonists in Rodents are Mediated via Distinct Receptor Subtypes. *J. Pharmacol. Exp. Ther.*
5
6
7 **2004**, *309*, 758-768.

8
9
10 (14) Sanna, M. G.; Liao, J.; Jo, E.; Alfonso, C.; Ahn, M.-Y.; Peterson, M. S.; Webb, B.;
11 Lefebvre, S.; Chun, J.; Gray, N.; Rosen, H. Sphingosine 1-Phosphate (S1P) Receptor
12 Subtypes S1P₁ and S1P₃, Respectively, Regulate Lymphocyte Recirculation and Heart Rate.
13
14
15
16 *J. Biol. Chem.* **2004**, *279*, 13839-13848.

17
18 (15) Koyrakh, L.; Roman, M. I.; Brinkmann, V.; Wickman, K. The Heart Rate Decrease
19 Caused by Acute FTY720 Administration is Mediated by the G Protein-Gated Potassium
20 Channel I_{KACH}. *Am. J. Transplant.* **2005**, *5*, 529-536.

21
22 (16) Gergeley, P.; Nuesslein-Hildesheim, B.; Guerini, D.; Brinkmann, V.; Traebert, M.;
23
24
25
26
27
28
29
30
31
32
33
34
35
36
37
38
39
40
41
42
43
44
45
46
47
48
49
50
51
52
53
54
55
56
57
58
59
60
Sing, T.; Luttringer, O.; Yang, J.; Gardin, A.; Wang, N.; Crumb Jr., W. J.; Saltzman, M.;
Rosenberg, M.; Wallström, E. The selective sphingosine 1-phosphate receptor modulator
BAF312 redirects lymphocyte distribution and has species-specific effects on heart rate. *Br.*
J. Pharmacol. **2012**, *167*, 1035-1047.

(17) Kunkel, G. T.; Maceyka, M.; Milstein, S.; Spiegel, S. Targeting the sphingosine-1-
phosphate axis in cancer, inflammation, and beyond. *Nat. Rev. Drug Disc.* **2013**, *12*, 688-702.

(18) Davis, M. D.; Clemens, J. J.; Macdonald, T. L.; Lynch, K. R. Sphingosine 1-Phosphate
Analogues as Receptor Antagonists. *J. Biol. Chem.* **2005**, *280*, 9833-9841.

(19) Wei, S. H.; Rosen, H.; Matheu, M. P.; Sanna, M. G.; Wang, S.-K.; Jo, E.; Wong, C.-H.;
Parker, I.; Cahalan, M. D. Sphingosine 1-phosphate type 1 receptor agonism inhibits
transendothelial migration of medullary T cells to lymphatic sinuses. *Nat. Immun.* **2005**, *6*,
1228-1235.

- 1
2
3 (20) Sanna, M. G.; Wang, S.-K.; Gonzalez-Cabrera, P. J.; Don, A.; Marsolais, D.; Matheu,
4 M. P.; Wei, S. H.; Parker, I.; Jo, E.; Chen, W.-C.; Cahalan, M. D.; Wong, C.-H.; Rosen, H.
5 Enhancement of capillary leakage and restoration of lymphocyte egress by a chiral S1P₁
6 antagonist in vivo. *Nat. Chem. Biol.* **2006**, *2*, 434-441.
7
8
9
10
11 (21) Fujii, Y.; Hirayama, T.; Ohtake, H.; Ono, N.; Inoue, T.; Sakurai, T.; Takayama, T.;
12 Matsumoto, K.; Tsukahara, N.; Hidano, S.; Harima, N.; Nakazawa, K.; Igarishi, Y.; Goitsuka,
13 R. Amelioration of Collagen-Induced Arthritis by a Novel S1P₁ Antagonist with
14 Immunomodulatory Activities. *J. Immunol.* **2012**, *188*, 206-215.
15
16
17
18
19
20 (22) Ibrahim, M. A.; Johnson, H. W. B.; Jeong, J. W.; Lewis, G. L.; Shi, X.; Noguchi, R. T.;
21 Williams, M.; Leahy, J. W.; Nuss, J. M.; Woolfrey, J.; Banica, M.; Bentzien, F.; Chou, Y.-C.;
22 Gibson, A.; Heald, N.; Lamb, P.; Mattheakis, L.; Matthews, D.; Shipway, A.; Wu, X.; Zhang,
23 W.; Zhou, S.; Shankar, G. Discovery of a Novel Class of Potent and Orally Bioavailable
24 Sphingosine 1-Phosphate Receptor 1 Antagonists. *J. Med. Chem.* **2012**, *55*, 1368-1381.
25
26
27
28
29
30 (23) Angst, D.; Janser, P.; Quancard, J.; Buehlmayer, P.; Berst, F.; Oberer, L.; Beerli, C.;
31 Streiff, M.; Pally, C.; Hersperger, R.; Bruns, C.; Bassilana, F.; Bollbuck, B. An Oral
32 Sphingosine 1-Phosphate Receptor 1 (S1P₁) Antagonist Prodrug with Efficacy in Vivo:
33 Discovery, Synthesis, and Evaluation. *J. Med. Chem.* **2012**, *55*, 9722-9734.
34
35
36
37
38
39 (24) Hennessy, E. J.; Grewal, G.; Byth, K.; Kamhi, V. M.; Li, D.; Lyne, P.; Oza, V.; Ronco,
40 L.; Rooney, M. T.; Saeh, J. C.; Su, Q. Discovery of Heterocyclic Sulfonamides as
41 Sphingosine 1-Phosphate Receptor 1 (S1P₁) Antagonists. *Bioorg. Med. Chem. Lett.* **2015**, *25*,
42 2041-2045.
43
44
45
46
47
48 (25) Oakley, R. H.; Hudson, C. C.; Cruickshank, R. D.; Meyers, D. M.; Payne Jr., R. E.;
49 Rhem, S. M.; Loomis, C. R. The Cellular Distribution of Fluorescently Labeled Arrestins
50 Provides a Robust, Sensitive, and Universal Assay for Screening G Protein-Coupled
51 Receptors. *ASSAY Drug Dev. Technol.* **2002**, *1*, 21-30.
52
53
54
55
56
57
58
59
60

- 1
2
3 (26) Leeson, P. D.; Springthorpe, B. The influence of drug-like concepts on decision-making
4 in medicinal chemistry. *Nat. Rev. Drug Disc.* **2007**, *6*, 881-890.
5
6
7 (27) Lin, J. H.; Lu, A. Y. H. Inhibition and Induction of Cytochrome P450 and the Clinical
8 Implications. *Clin. Pharmacokinet.* **1998**, *35*, 361-390.
9
10
11 (28) Kocarek, T. A.; Schuetz, E. G.; Strom, S. C.; Fisher, R. A.; Guzelian, P. S. Comparative
12 Analysis of Cytochrome P4503A Induction in Primary Cultures of Rat, Rabbit, and Human
13 Hepatocytes. *Drug Metab. Dispos.* **1995**, *23*, 415-421.
14
15
16 (29) Jones, S. A.; Moore, L. B.; Shenk, J. L.; Wisely, G. B.; Hamilton, G. A.; McKee, D. D.;
17 Tomkinson, N. C. O.; LeCluyse, E. L.; Lambert, M. H.; Willson, T. M.; Kliewer, S. A.;
18 Moore, J. T. The Pregnane X Receptor: A Promiscuous Xenobiotic Receptor That Has
19 Diverged during Evolution. *Mol. Endocrinol.* **2000**, *14*, 27-39.
20
21
22 (30) Burk, O.; Koch, I.; Raucy, J.; Hustert, E.; Eichelbaum, M.; Brockmöller, J.; Zanger, U.
23 M.; Wojnowski, L. The Induction of Cytochrome P450 3A5 (CYP3A5) in the Human Liver
24 and Intestine Is Mediated by the Xenobiotic Sensors Pregnane X Receptor (PXR) and
25 Constitutively Activated Receptor (CAR). *J. Biol. Chem.* **2004**, *279*, 38379-38385.
26
27
28 (31) Bertilsson, G.; Heidrich, J.; Svensson, K.; Åsman, M.; Jendeberg, L.; Sydow-Bäckman,
29 M.; Ohlsson, R.; Postlind, H.; Blomquist, P.; Berkenstam, A. Identification of a human
30 nuclear receptor defines a new signaling pathway for *CYP3A* induction. *Proc. Natl. Acad. Sci.*
31 *USA* **1998**, *95*, 12208-12213.
32
33
34 (32) Lehmann, J. M.; McKee, D. D.; Watson, M. A.; Willson, T. M.; Moore, J. T.; Kliewer, S.
35 A. The Human Orphan Nuclear Receptor PXR Is Activated by Compounds That Regulate
36 *CYP3A4* Gene Expression and Cause Drug Interactions. *J. Clin. Invest.* **1998**, *102*, 1016-
37 1023.
38
39
40 (33) Kliewer, S. A.; Moore, J. T.; Wade, L.; Staudinger, J. L.; Watson, M. A.; Jones, S. A.;
41 McKee, D. D.; Oliver, B. B.; Willson, T. M.; Zetterström, R. H.; Perlmann, T.; Lehmann, J.
42
43
44
45
46
47
48
49
50
51
52
53
54
55
56
57
58
59
60

1
2
3 M. An Orphan Nuclear Receptor Activated by Pregnanes Defines a Novel Steroid Signaling
4
5 Pathway. *Cell* **1998**, *92*, 73-82.

6
7 (34) Baes, M.; Gulick, T.; Choi, H.-S.; Martinoli, M. G.; Simha, D.; Moore, D. D. A New
8
9 Orphan Member of the Nuclear Hormone Receptor Superfamily That Interacts with a Subset
10
11 of Retinoic Acid Response Elements. *Mol. Cell. Biol.* **1994**, *14*, 1544-1552.

12
13 (35) Raucy, J.; Warfe, L.; Yueh, M.-F.; Allen, S. W. A Cell-Based Reporter Gene Assay for
14
15 Determining Induction of CYP3A4 in a High-Volume System. *J. Pharmacol. Exp. Ther.*
16
17 **2002**, *303*, 412-423.

18
19 (36) Lemaire, G.; de Sousa, G.; Rahmani, R. A PXR reporter gene assay in a stable cell
20
21 culture system: CYP3A4 and CYB2B6 induction by pesticides. *Biochem. Pharmacol.* **2004**,
22
23 *68*, 2347-2358.

24
25 (37) Gao, Y.-D.; Olson, S. H.; Balkovec, J. M.; Zhu, Y.; Royo, I.; Yabut, J.; Evers, R.; Tan,
26
27 E. Y.; Tang, W.; Hartley, D. P.; Mosley, R. T. Attenuating pregnane X receptor (PXR)
28
29 activation: A molecular modelling approach. *Xenobiotica* **2007**, *37*, 124-138.

30
31 (38) Salonen, L. M.; Ellermann, M.; Diederich, F. Aromatic Rings in Chemical and
32
33 Biological Recognition: Energetics and Structures. *Angew. Chem., Int. Ed. Engl.* **2011**, *50*,
34
35 4808-4842.

36
37 (39) Bjornsson, T. D.; Callaghan, J. T.; Einolf, H. J.; Fischer, V.; Gan, L.; Grimm, S.; Kao, J.;
38
39 King, S. P.; Miwa, G.; Ni, L.; Kumar, G.; McLeod, J.; Obach, R. S.; Roberts, S.; Roe, A.;
40
41 Shah, A.; Snikeris, F.; Sullivan, J. T.; Tweedie, D.; Vega, J. M.; Walsh, J.; Wrighton, S. A.
42
43 The Conduct of in vitro and in vivo Drug-Drug Interaction Studies: A Pharmaceutical
44
45 Research and Manufacturers of America (PhRMA) Perspective. *Drug Metab. Dispos.* **2003**,
46
47 *31*, 815-832.

48
49 (40) Luo, G.; Cunningham, M.; Kim, S.; Burn, T.; Lin, J.; Sinz, M.; Hamilton, G.; Rizzo, C.;
50
51 Jolley, S.; Gilbert, D.; Downey, A.; Mudra, D.; Graham, R.; Carroll, K.; Xie, J.; Madan, A.;
52
53
54
55
56
57
58
59
60

1
2
3 Parkinson, A.; Christ, D.; Selling, B.; Lecluyse, E.; Gan, L.-S. CYP3A4 Induction by Drugs:
4
5 Correlation Between a Pregnane X Receptor Reporter Gene Assay and CYP3A4 Expression
6
7 in Human Hepatocytes. *Drug Metab. Dispos.* **2002**, *30*, 795-804.

8
9
10 (41) Lee, M.-J.; Thangada, S.; Claffey, K. P.; Ancellin, N.; Liu, C. H.; Kluk, M.; Volpi, M.;
11
12 Sha'afi, R. I.; Hla, T. Vascular Endothelial Cell Adherens Junction Assembly and
13
14 Morphogenesis Induced by Sphingosine-1-Phosphate. *Cell* **1999**, *99*, 301-312.

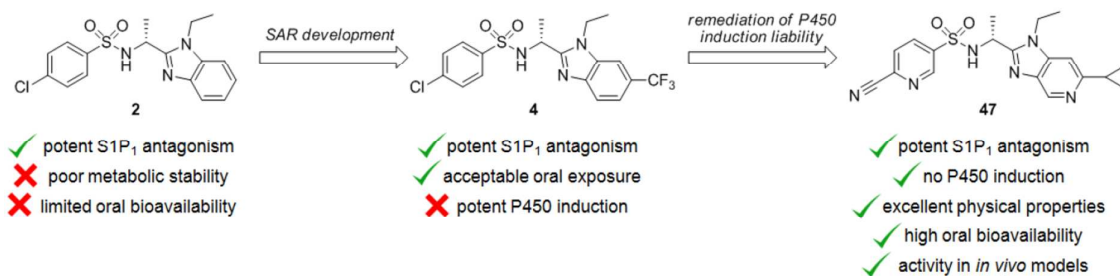
15
16 (42) Foss, Jr., F. W.; Snyder, A. H.; Davis, M. D.; Rouse, M.; Okusa, M. D.; Lynch, K. R.;
17
18 Macdonald, T. L. Synthesis and biological evaluation of γ -aminophosphonates as potent,
19
20 subtype-selective sphingosine 1-phosphate receptor agonists and antagonists. *Bioorg. Med.*
21
22 *Chem.* **2007**, *15*, 663-677.

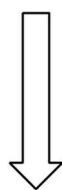
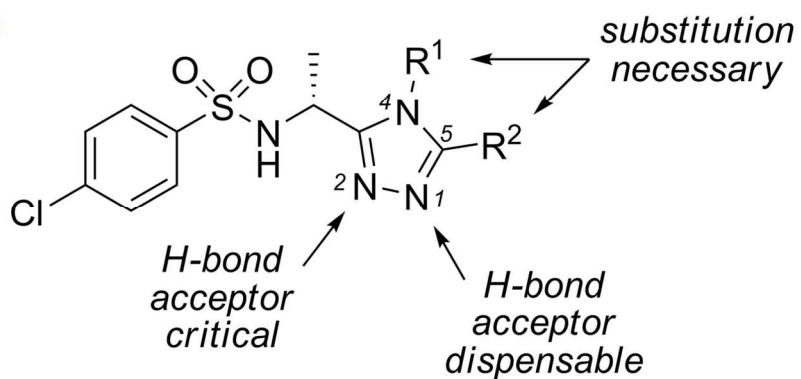
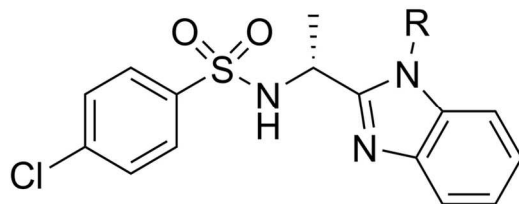
23
24
25 (43) Wedge, S. R.; Kendrew, J.; Hennequin, L. F.; Valentine, P. J.; Barry, S. T.; Brave, S. R.;
26
27 Smith, N. R.; James, N. H.; Dukes, M.; Curwen, J. O.; Chester, R.; Jackson, J. A.; Boffey, S.
28
29 J.; Kilburn, L. L.; Barnett, S.; Richmond, G. H. P.; Wadsworth, P. F.; Walker, M.; Bigley, A.
30
31 L.; Taylor, S. T.; Cooper, L.; Beck, S.; Jürgensmeier, J. M.; Ogilvie, D. J. AZD2171: A
32
33 Highly Potent, Orally Bioavailable, Vascular Endothelial Growth Factor Receptor-2 Tyrosine
34
35 Kinase Inhibitor for the Treatment of Cancer. *Cancer Res.* **2005**, *65*, 4389-4400.

36
37
38 (44) Smith, N. R.; James, N. H.; Oakley, I.; Wainwright, A.; Copley, C.; Kendrew, J.;
39
40 Womersley, L. M.; Jürgensmeier, J. M.; Wedge, S. R.; Barry, S. T. Acute pharmacodynamic
41
42 and antivascular effects of the vascular endothelial growth factor signaling inhibitor
43
44 AZD2171 in Calu-6 human lung tumor xenografts. *Mol. Cancer Ther.* **2007**, *6*, 2198-2208.

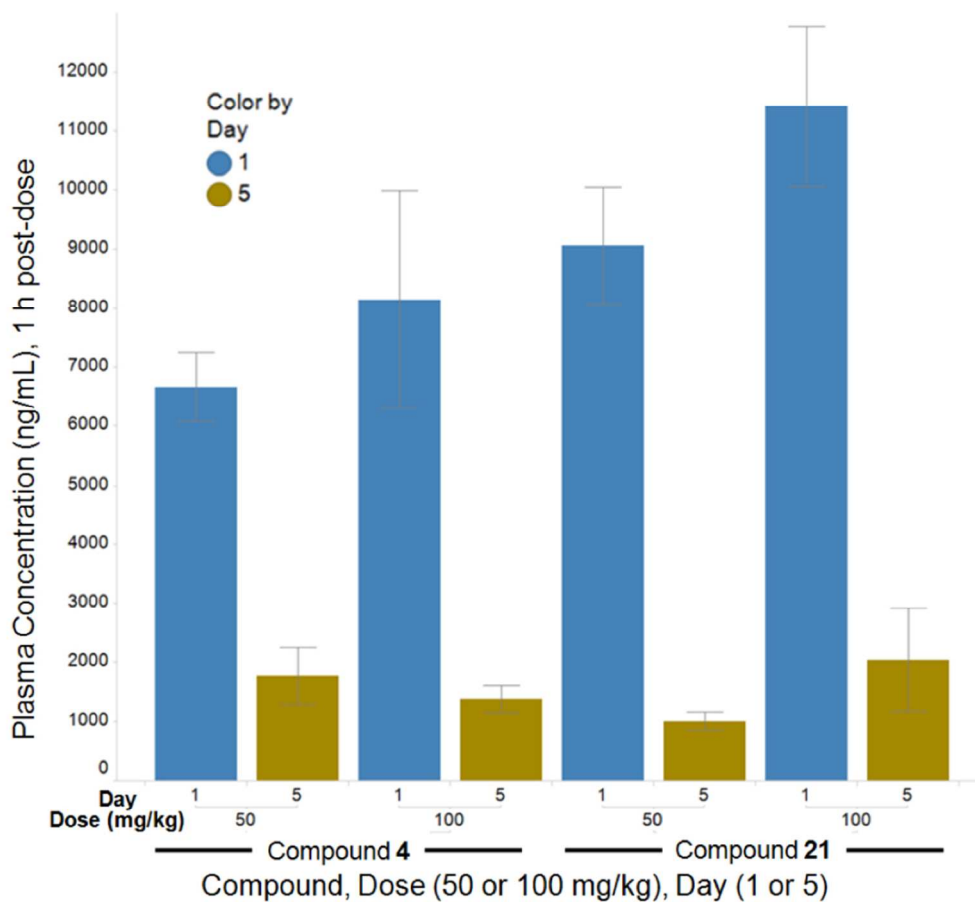
45
46
47 (45) Makosza, M.; Sienkiewicz, K. Hydroxylation of Nitroarenes with Alkyl Hydroperoxide
48
49 Anions via Vicarious Nucleophilic Substitution of Hydrogen. *J. Org. Chem.* **1998**, *63*, 4199-
50
51 4208.
52
53
54
55
56
57
58
59
60

Table of Contents graphic

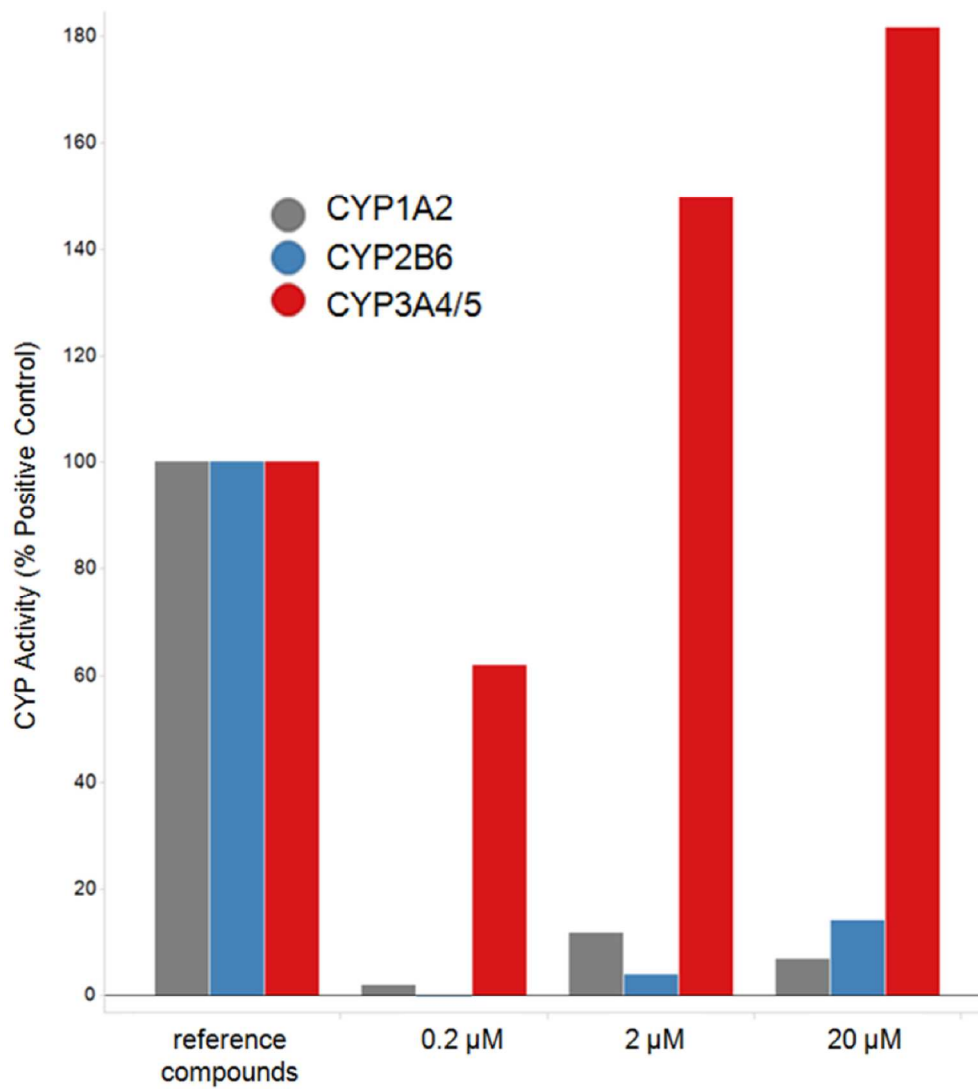


Triazole**scaffold hopping****Benzimidazole**

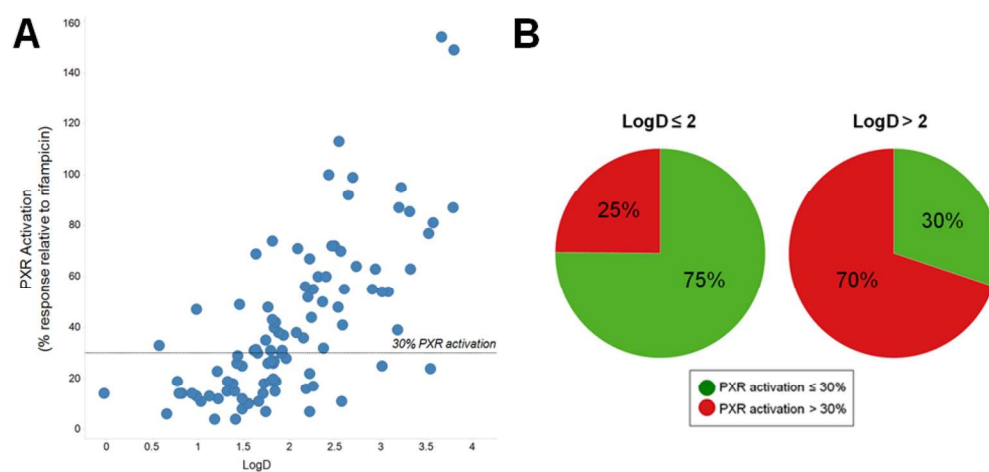
65x56mm (600 x 600 DPI)



84x76mm (300 x 300 DPI)

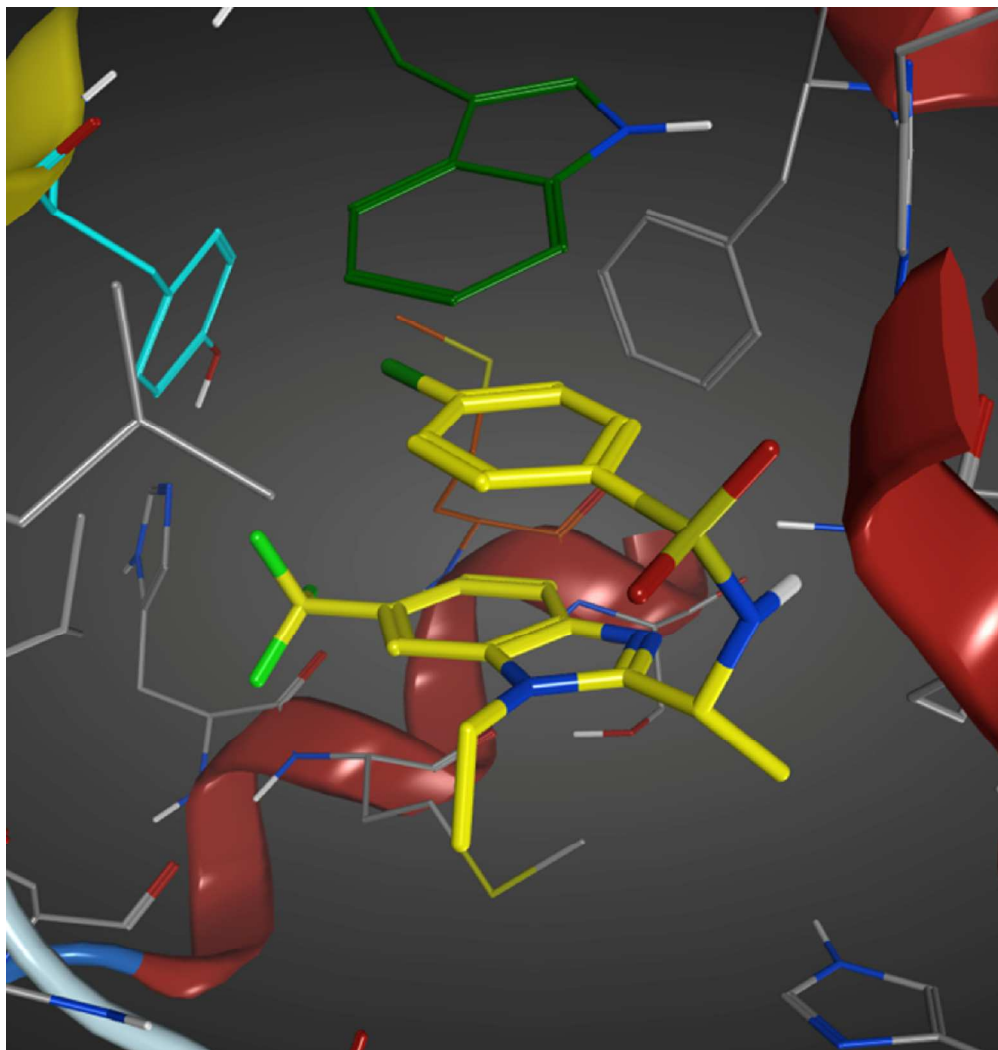


84x92mm (300 x 300 DPI)

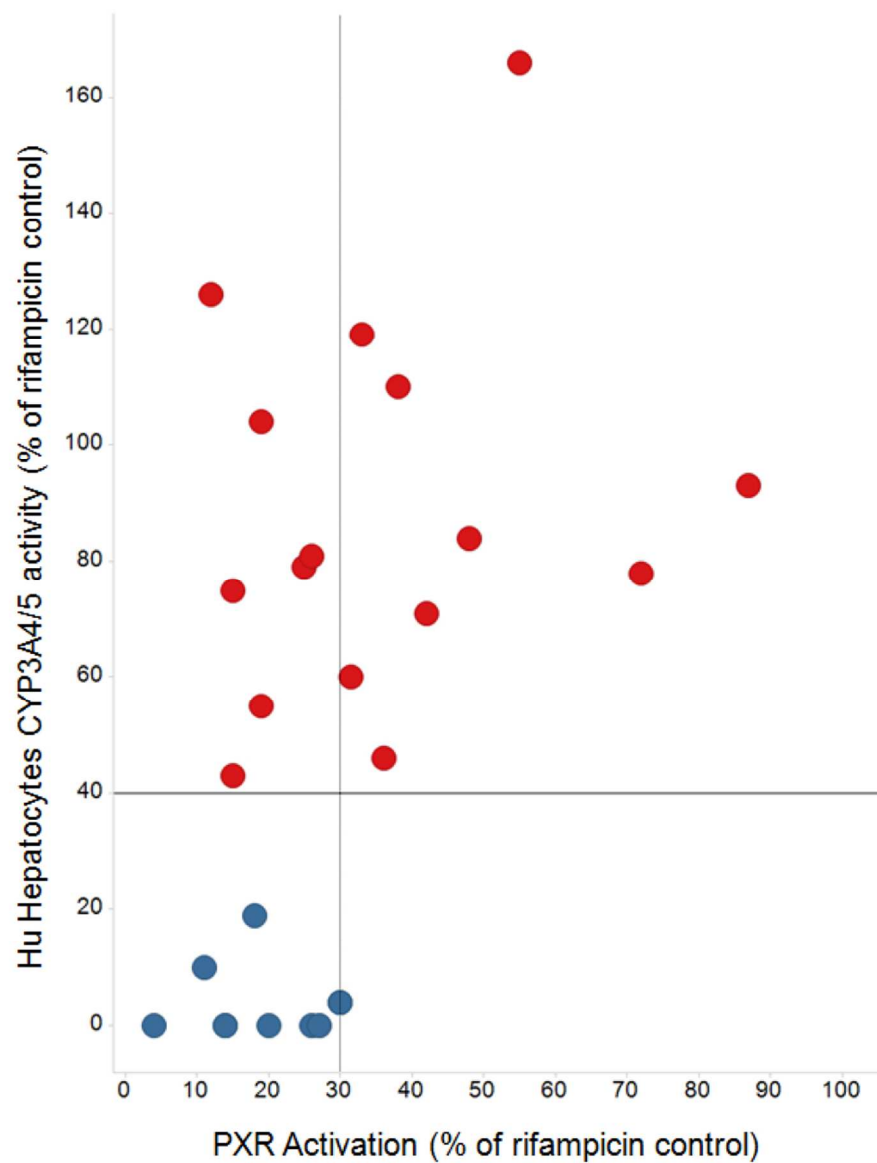


176x85mm (300 x 300 DPI)

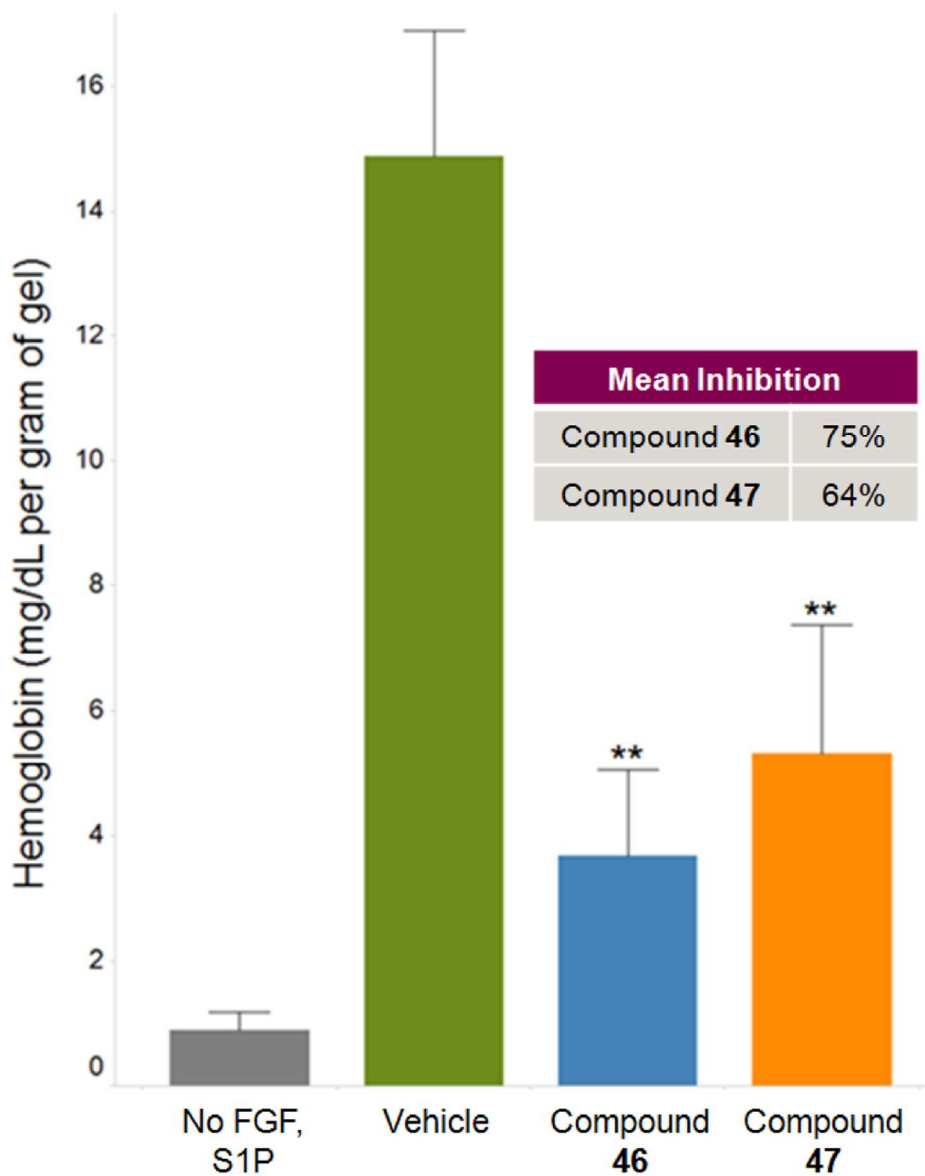
1
2
3
4
5
6
7
8
9
10
11
12
13
14
15
16
17
18
19
20
21
22
23
24
25
26
27
28
29
30
31
32
33
34
35
36
37
38
39
40
41
42
43
44
45
46
47
48
49
50
51
52
53
54
55
56
57
58
59
60

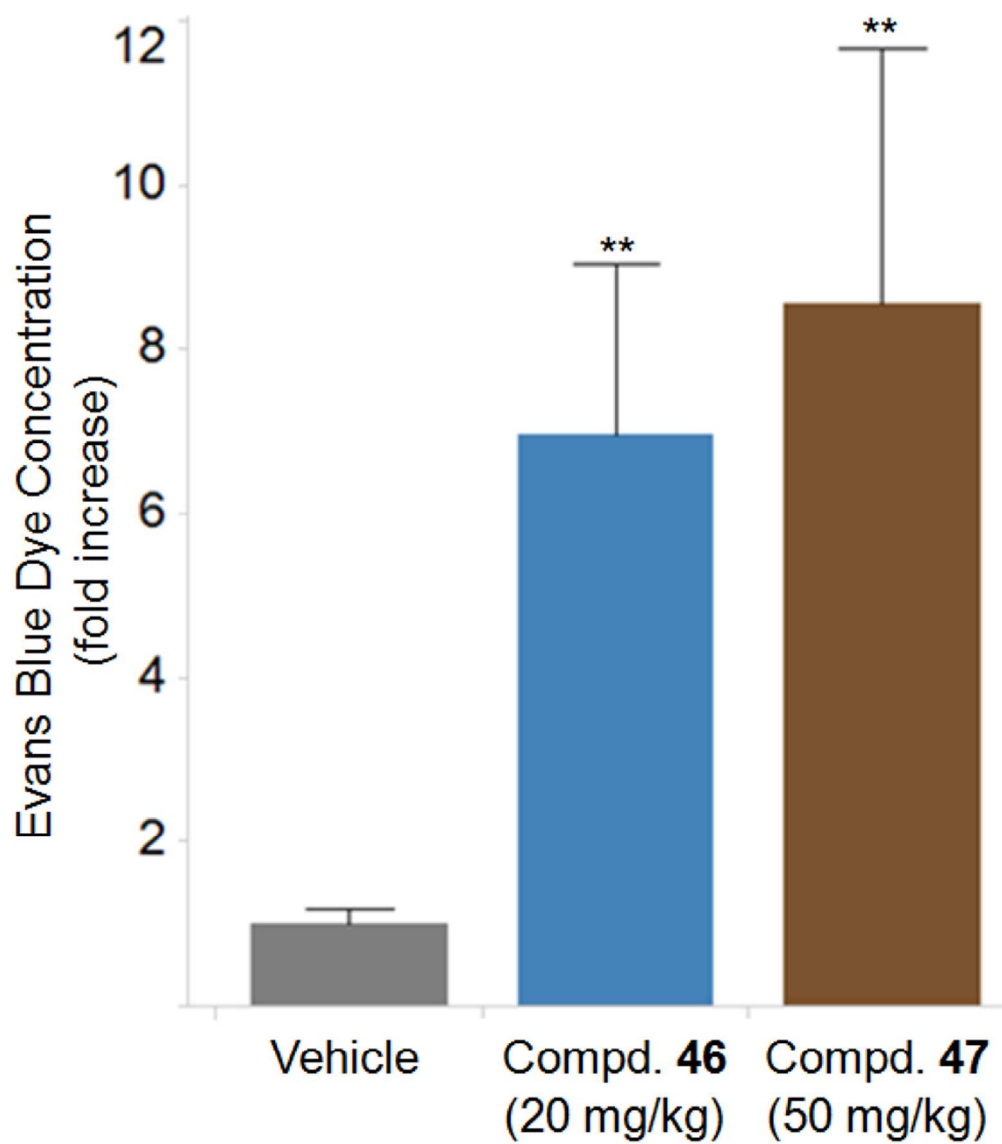


83x86mm (300 x 300 DPI)

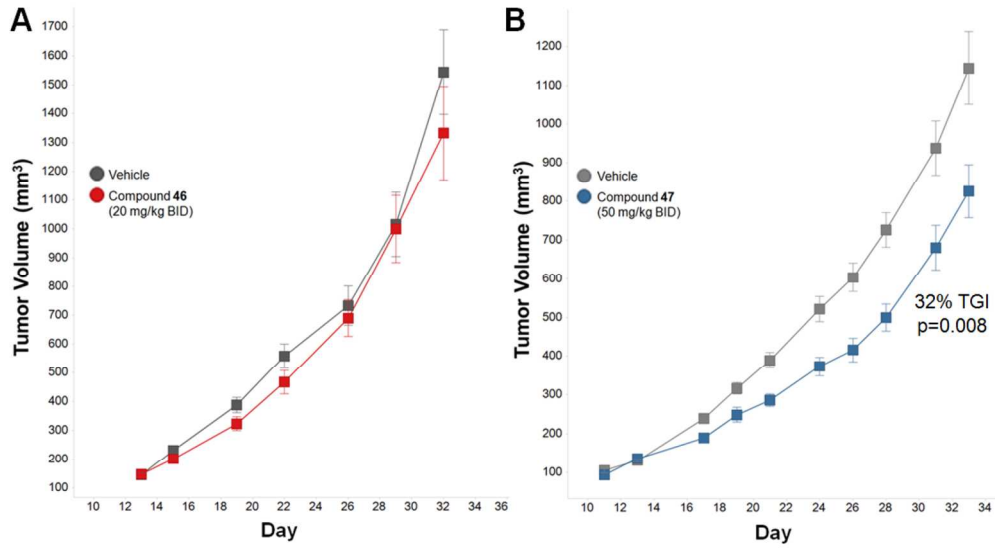


83x113mm (300 x 300 DPI)

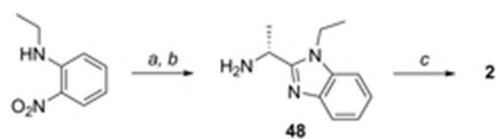




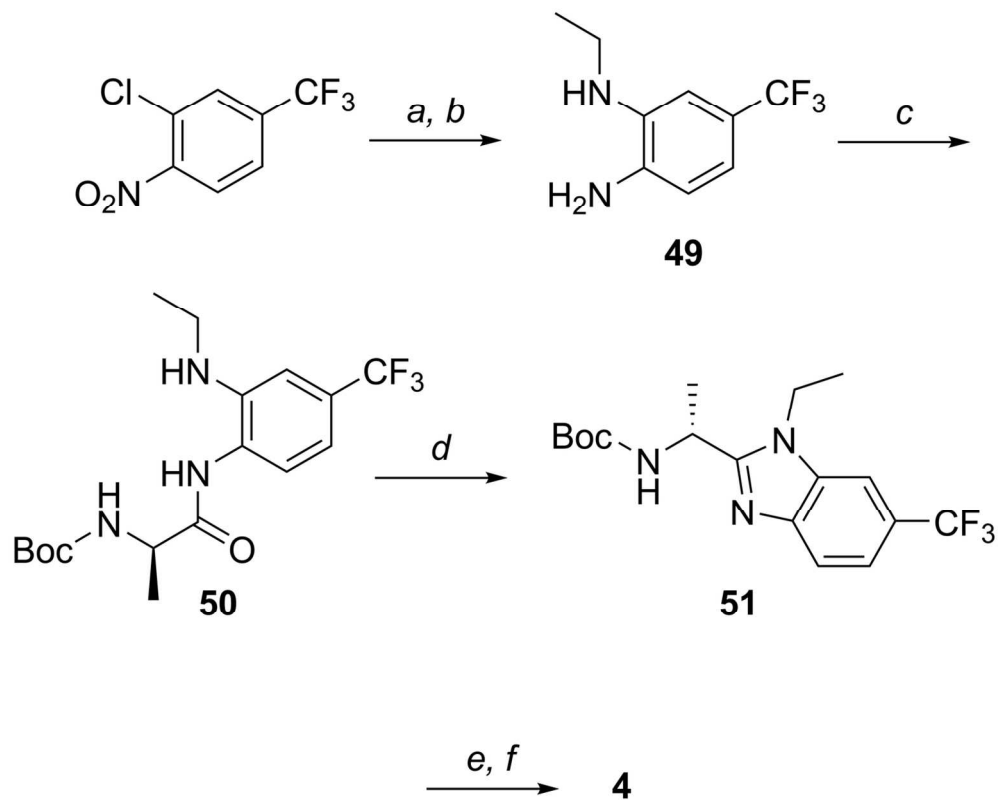
82x97mm (300 x 300 DPI)



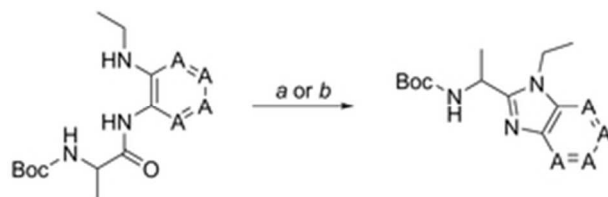
175x97mm (300 x 300 DPI)



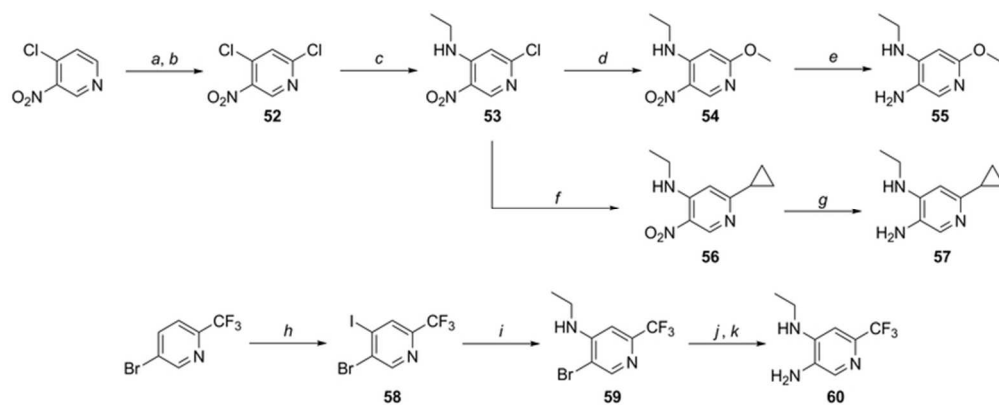
20x5mm (300 x 300 DPI)



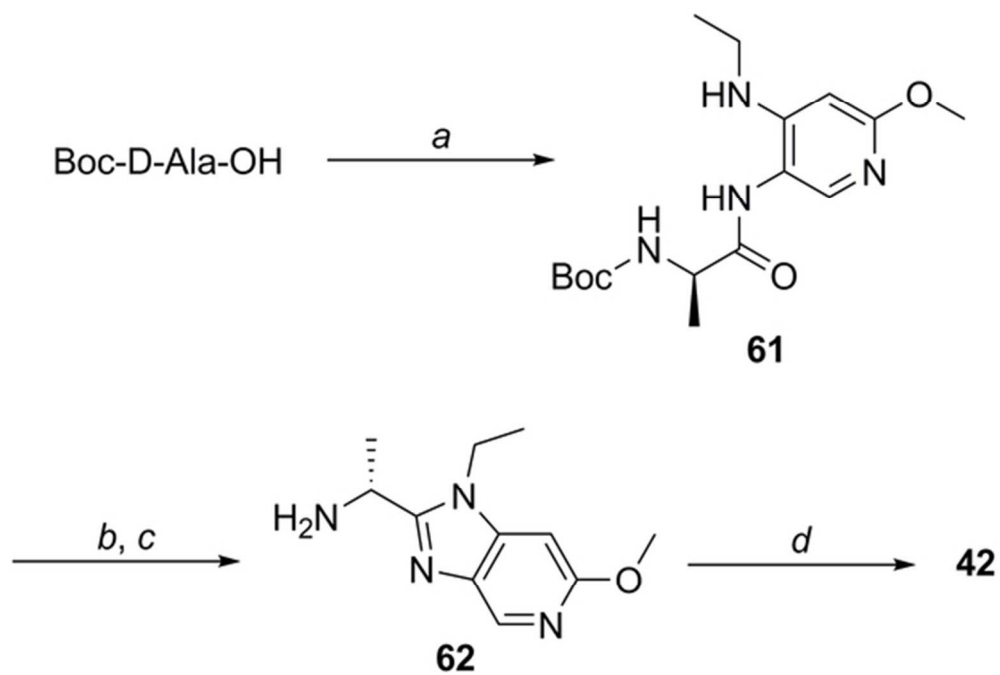
64x51mm (600 x 600 DPI)



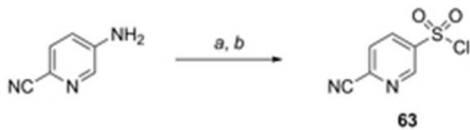
25x8mm (300 x 300 DPI)



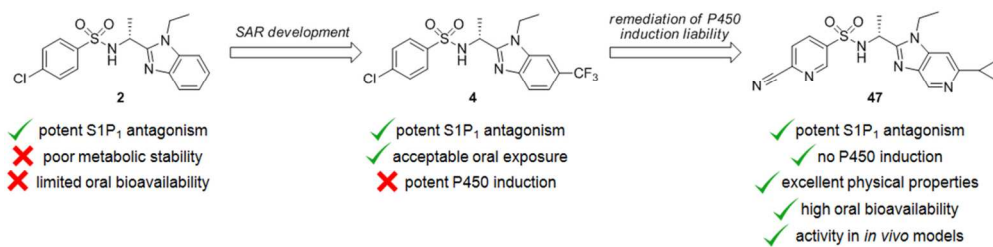
69x27mm (300 x 300 DPI)



52x35mm (300 x 300 DPI)



19x5mm (300 x 300 DPI)



54x14mm (600 x 600 DPI)